Chem Soc Rev

REVIEW ARTICLE

View Article Online
View Journal | View Issue

Cite this: *Chem. Soc. Rev.*, 2017, **46**, 2497

Anion transport and supramolecular medicinal chemistry

Philip A. Gale *[a] Jeffery T. Davis *[b] and Roberto Quesada *[c]

Received 1st March 2017

DOI: 10.1039/c7cs00159b

rsc.li/chem-soc-rev

New approaches to the transmembrane transport of anions are discussed in this review. Advances in the design of small molecule anion carriers are reviewed in addition to advances in the design of synthetic anion channels. The application of anion transporters to the potential future treatment of disease is discussed in the context of recent findings on the selectivity of anion transporters.

Introduction

Ion transport across biological membranes is an important process, regulated by membrane-embedded pumps, channels and carriers, that maintains ion and pH homeostasis in cells.[1] Genetic diseases can result in dysregulated ion transport due to perturbations in the structure of ion channels.[2] These diseases, such as cystic fibrosis (CF) caused by the dysfunction of the cystic fibrosis transmembrane conductance regulator (CFTR),[3] are collectively known as channelopathies.[4]

The development of synthetic carriers and transmembrane channels has been driven to some degree by the potential application of these supramolecular constructs in the treatment of diseases caused by dysregulated anion transport. Many groups have used model membrane systems often employing vesicles composed of lipid or lipid/cholesterol mixtures as test beds for the efficacy of synthetic transporters. Excitingly, more recently, groups have begun to explore the anion transport properties of synthetic ionophores in cells. Supramolecular medicinal

[a] *School of Chemistry (F11), The University of Sydney, 2006 NSW, Australia. E-mail: philip.gale@sydney.edu.au*
[b] *Department of Chemistry and Biochemistry, University of Maryland, College Park, MD 20742, USA. E-mail: jdavis@umd.edu*
[c] *Departmento de Química, Universidad de Burgos, 09001 Burgos, Spain. E-mail: rquesada@ubu.es*

Philip A. Gale

Philip A. Gale is Professor and Head of the School of Chemistry at the University of Sydney. Phil's research interests focus on the supramolecular chemistry of anionic species and in particular the molecular recognition, sensing and lipid bilayer transport of anions. Phil has won a number of research prizes for this work including the RSC 2014 Supramolecular Chemistry Award, a Royal Society Wolfson Research Merit Award, the RSC Corday Morgan medal and prize and the RSC Bob Hay Lectureship.

Jeffery T. Davis

Jeffery T. Davis, born and raised in the Berkshires of Western Massachusetts, received his BA degree in Chemistry in 1981 from Colby College in Waterville, Maine. He earned a PhD in Organic Chemistry from MIT in 1987, under the guidance of Professor Satoru Masamune. For the next 3 years he was Group Leader of Bioorganic Chemistry at Genzyme Corp. in Boston. From 1990–1993 he was an NIH postdoctoral fellow, training in biomolecular NMR, with Professor Brian Reid at the University of Washington. In 1993 he joined the faculty in the Department of Chemistry and Biochemistry at the University of Maryland in College Park. His research group works on problems in supramolecular self-assembly, G-quadruplex structure and function and transmembrane ion transport.

chemistry[5] – the development of supramolecular systems to function in biological systems with therapeutic benefit – is still at an early stage. Encouragingly anion transporters have been shown to be capable of transporting chloride through epithelial cell membranes – effectively replacing the function of faulty CFTR channels. pH gradient dissipation is often observed within cells upon exposure to anion transporters and recent work has elucidated the mechanism of this process which often leads to apoptosis. Hence anion transporters also have potential application in the treatment of cancer and natural products, such as the prodigiosins and synthetic analogues capable of H^+/Cl^- transport, have been studied extensively in this regard.

This tutorial review will cover recent progress in anion transporter design including new hydrogen bonding anionophores and systems that use non-classical interactions such as halogen bonding to complex and transport anionic substrates. We will also look at recent developments in the design and synthesis of synthetic channels and pores and also progress in optimising transport mediated by small molecules. New assays for monitoring anion transport and measuring selectivity in transport will also be discussed.

Synthetic hydrogen bond donors

Calix[4]pyrrole macrocycles have demonstrated great versatility as platforms to develop transmembrane ion transporters. These macrocycles are capable of binding both anions and large, polarizable cations through the pyrrolic N–H groups and the aromatic cup respectively. Early studies showed the ability of *meso*-octamethylcalix[4]pyrrole **1** to promote CsCl transmembrane co-transport (symport). Co-transport or symport is the process in which two ions are transported together across a lipid bilayer. In the case of compound **1** the macrocycle functions as an electroneutral CsCl co-transporter as the overall transport process does not result in a net flow of charge across the membrane. Gale, Sessler *et al.* studied the parent *meso*-octamethyloctafluorocalix[4]pyrrole **2**.[6] Fluorination of the pyrrole rings was found to enhance the acidity of the NH hydrogen bond donor groups leading to stronger $NH\cdots Cl^-$ interactions and dramatically change the transmembrane transport activity of the molecule. Thus compound **2** proved to be an efficient anion exchanger, promoting nitrate/chloride exchange in 1-palmitoyl-2-oleoyl-*sn*-*glycero*-3-phosphocholine (POPC) vesicles irrespective of the MCl (M = Li, Na, K, Rb, Cs) salt employed. This compound also facilitated bicarbonate/chloride exchange. Therefore, the presence of the electron-withdrawing fluorine substituents induces a change from CsCl co-transporter as predominant transport mechanism for **1** to a much more potent anion exchanger capable of anion uniport for **2**. Uniport is the simple transport of one species across a membrane – in the case of compound **2** it is capable of chloride uniport in the absence of caesium cations. Strapped calix[4]pyrroles **3–6**, bearing triazole groups that contribute to enhance the chloride binding affinity were studied by Gale.[7] Chloride efflux from POPC liposomes was measured using several chloride salts. In all cases, higher chloride efflux was observed in the chloride/nitrate exchange assay using caesium salts. This result highlighted the contribution of both MCl co-transport and anion exchange to the transport activity displayed by these compounds. The length of the alkyl chain of the bis-triazole strap was found to be very important in the extent of chloride efflux, with compound **6** being the most effective (Fig. 1).

The binding and transport properties of an oligoether-strapped calix[4]pyrrole **7** were studied by Gale, Sessler and Lee (Fig. 2).[8] This compound formed stable 1 : 1 ion-pair complexes with LiCl and NaCl. Chloride selective electrode assays in POPC liposomes showed that **7** can function both as a chloride/nitrate exchanger as well as M^+/Cl^- co-transporter, preferentially for caesium cations.

Simple bis-indolylurea derivatives **8–16** were studied by Gale and colleagues.[9] The two anion binding units were linked

Roberto Quesada

Roberto Quesada was born and raised in Asturias, in the north of Spain. He obtained his PhD degree in 2002 at the University of Oviedo under the guidance of Prof. Javier Ruiz. After post-doctoral appointments at the Trinity College Dublin and the University of Southampton he was awarded with a "Juan de la Cierva" contract in the group of Prof. Pilar Prados at the Universidad Autónoma de Madrid in 2006. In 2008 he moved to the University of Burgos as "Ramon y Cajal" Fellow and became "profesor titular" in 2012. His research interests include synthetic and supramolecular chemistry, with a focus in biological applications.

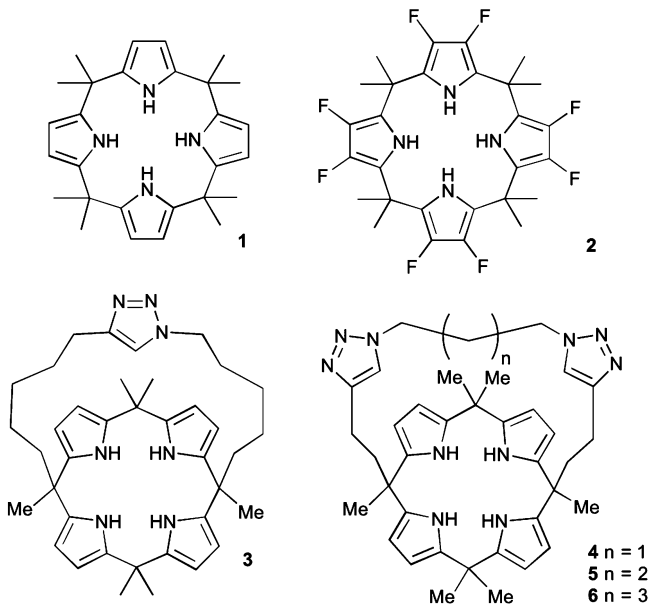

Fig. 1 Calix[4]pyrrole derivatives **1–6**.

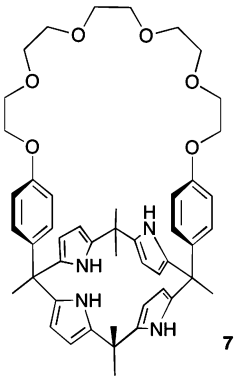

Fig. 2 Strapped calix[4]pyrrole **7**.

through flexible alkyl chains of different length. Despite the lack of cooperativity of the binding sites, these compounds were found to function as effective anion transporters, outperforming the parent mono-indolylurea derivatives. The relative transport activity could be modulated by choosing the appropriate alkyl linker, which has a direct impact on the overall lipophilicity of the transporter. Molecular dynamics simulations in the POPC bilayer model indicated that the structure of the lipid bilayer is not disturbed by the internalization of these compounds and the average distance that a molecule travels inside the membrane was reduced for the longer transporter, which is in agreement with the lower activity of this compound.

The same group introduced squaramide-based compounds such as derivatives **17–19** as transmembrane anion transporters.[10] These compounds outperformed analogous ureas and thioureas in terms of transmembrane transport activity. Using POPC liposomes, these compounds proved extremely efficient transporters promoting both nitrate/chloride exchange and bicarbonate/chloride exchange, with EC_{50} values (the effective concentration of transporter to achieve 50% anion efflux at a particular time in the experiment) down to 0.01% transporter : lipid molar ratio in the case of nitrate/chloride exchange facilitated by **19**. The analogous oxothiosquaramide **20** was also developed and studied by Gale, Jolliffe and colleagues.[11] The transmembrane anion transport abilities of this oxothiosquaramide were investigated in liposomes and it was found that it functions as mobile carrier that can promote chloride efflux mainly *via* chloride/nitrate exchange process, although HCl symport can also occur in the presence of a pH gradient. This compound is significantly more acidic than regular squaramides, with pK_a values around 6. Thus at pH 7.2 the anion transport ability of **20** is fully switched OFF due to deprotonation of the receptor, but the activity is switched ON at lower pH. Gale's group have also provided another remarkable example of a pH switchable transporter.[12] Phenylthiosemicarbazones can be protonated at acidic pH and function as a highly active H^+/Cl^- cotransporters. For instance, the calculated EC_{50} for compound **21** in the chloride/nitrate assay at pH 4.0 was 0.0074 mol%. This value is 640-times lower than that observed at pH of 7.2. Thus, this system represents an example of a non-electrogenic (or electroneutral) transporter (a transporter that does not facilitate a net flow of

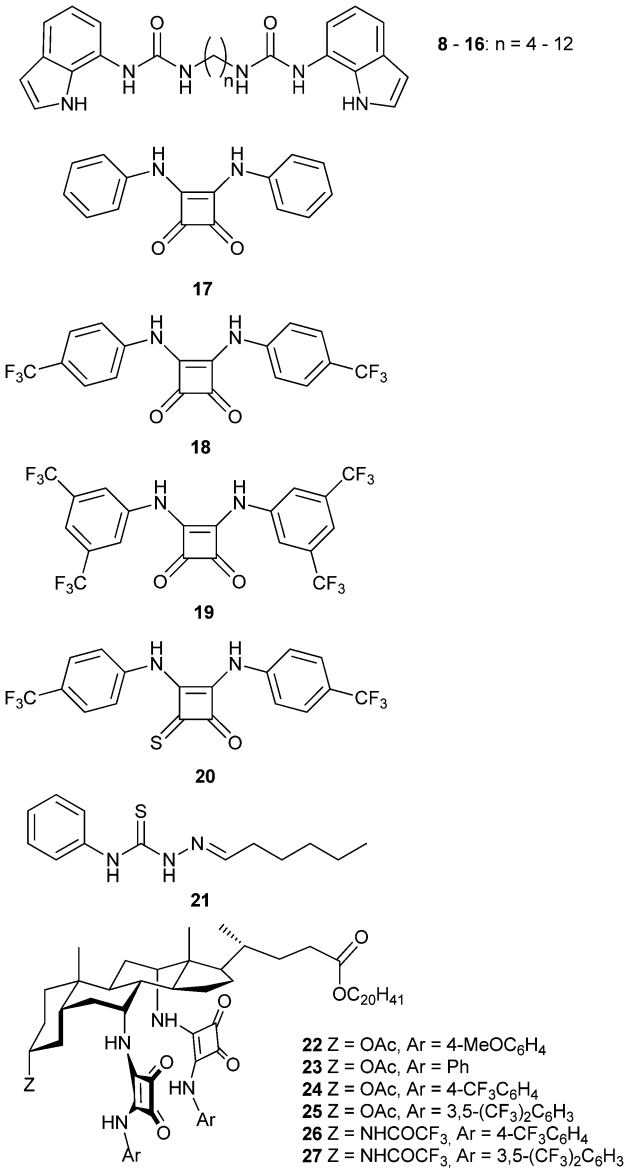

Fig. 3 Urea-thiosemicarbazone- and squaramide-containing derivatives **8–27**.

charge as – in this case – both a H^+ and Cl^- are transported) displaying pH-switching behaviour between acidic and neutral pH conditions. This pH switchable activity has potential useful implications in biological studies, targeting for instance chloride transport in acidic organelles (Fig. 3).

Squaramide binding motifs were also appended to the axial positions of steroid-based anion receptors (compounds **22–27**, Fig. 3) by Gale and A. P. Davis.[13] Steroid structures (in particular cholic acid derivatives) are lipophilic motifs developed by A. P. Davis's group as lipophilic scaffolds from which anion transporters may be constructed. In this case, the steroid framework with squaramide binding units resulted in extremely high affinities for tetra-alkylammonium salts of anions in chloroform. These compounds were found to be active transporters in POPC liposomes at loadings of receptor/lipid = 1 : 2500 by the lucigenin

method (lucigenin's fluorescence is collisionally quenched by halide anions allowing transmembrane transport to be followed by fluorescence measurements).[14] This activity is significantly lower than that found in thiourea decorated steroid-based anion receptors. This result could suggest that the affinity of these squaramide derivatives was too high and decomplexation of the anions is likely limiting the transmembrane transport activity of these compounds.

Channels and pores

Protein channels that span the bilayer membrane provide a conduit for charged ions to cross that hydrophobic barrier. Defects in these channel proteins can lead to serious diseases, such as cystic fibrosis. One strategy for combating such "channelopathies" would be to use a synthetic compound that could arrange in the bilayer membrane so as to mimic the structure and function of an anion channel. In the past 5–6 years there have been a number of synthetic channels designed for the specific purpose of catalysing the transmembrane transport of anions. Most of these synthetic anion channels have been formed by self-assembly of molecular building blocks within the lipid membrane. The ultimate proof of an ion channel is usually taken to be the "open–closed" ion conductances shown in voltage clamp experiments on planar bilayers. The interpretation is that this conductance is due to the dynamic self-assembly of subunits within the membrane. When an active structure is formed by self-assembly then a transient pathway is formed that enables anion conductance across the membrane.

Gokel and colleagues described a series of low molecular weight isophthalamides and pyridine analogues that functioned as transmembrane Cl^- transporters in POPC vesicles.[15] While most of the compounds described in the paper were mobile carriers and not channel formers, 4,4′-dinitropicolinanilide **28** (m.w. 407) showed properties characteristic of a functional ion channel (Fig. 4) at voltages that are physiologically relevant. The most convincing evidence for channel formation by **28** was its hallmark "open–closed" conductance activity in planar bilayer experiments. The authors found that the most frequently observed conductance state corresponded to a pore size of *ca.* 8 Å, close to the diameter of a hydrated Cl^- anion (6.5 Å). To function as a channel, the small molecule **28** would have to self-assemble into an ordered pore within the hydrophobic membrane. Gokel and colleagues suggested that **28** self-assembles *via* π–π interactions between individual subunits. In support of such a mechanism the authors offered 3 pieces of evidence. First, an X-ray crystal structure of **28** shows that it forms π–π stacks in the solid-state. Second, fluorescence spectra of **28** in the presence of 0.17 mM DOPC vesicles showed formation of an excimer peak that the authors proposed formed upon self-association in the lipid membrane. Finally, using data from anion transport studies in POPC vesicles, the authors found that 4,4′-dinitropicolinanilide **28** transported Cl^- with a Hill coefficient of >1 at relatively high concentrations of added transporter. Such a value for the Hill coefficient

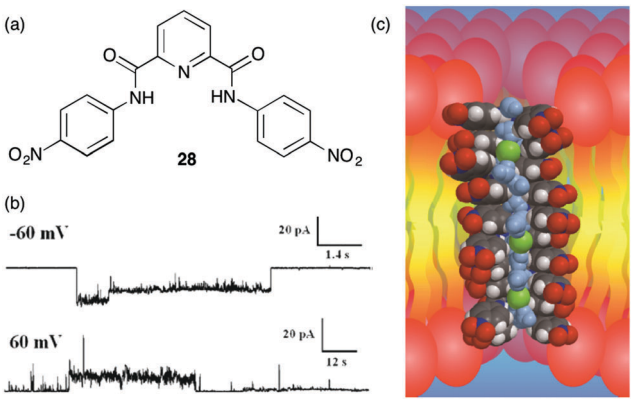

Fig. 4 Transmembrane chloride transport by (a) 4,4′-dinitropicolinamide **28** appears to occur *via* a channel mechanism: (b) the current observed at applied voltages of −60 mV and +60 mV upon addition of transporter **28** to a planar bilayer (c) DFT-calculated molecular model showing a stack of 10 molecules of **28**, 3 chloride anions and 16 water molecules. The distance between the most distal monomers in the stack is approximately 34 Å. Reproduced from ref. 15. Copyright 2010, Royal Society of Chemistry.

would indicate that multiple monomers come together to form the active transporter. Gokel and colleagues built an energy-minimized model of the channel by stacking triarenes in a face-to-face orientation; they proposed that this "semi-organized" array of stacked hydrogen bond sites could catalyse transmembrane transport of Cl^- anions. They suggested that sliding or rotation of an individual monomer **28** out of the stacked array could account for the "open–closed" conductance observed in the bilayer conductance experiments. Even though the proposed channel structure is speculative this study nicely highlights how self-assembly of low molecular weight building blocks can be a powerful strategy for construction of synthetic anion channels that function in lipid membranes.

Recently, Gong and colleagues have extended this self-assembly strategy to form transmembrane ion channels from aromatic oligoamide macrocycles, such as **29-H** and **29-NH_2**.[16] The authors hypothesized that a transmembrane pore would form if about 10 macrocycles stacked one on another to give a nanotube of *ca.* 34 Å, a distance matching the thickness of the hydrophobic portion of the bilayer membrane. Furthermore such a nanotube, formed by self-assembly of macrocycles **29**, would also contain *ca.* 10 functional groups on its inner surface. The authors reasoned that the identity of these functional groups (shown as X in Fig. 5) on the channel's interior might well influence their ion selectivity.

Both **29-H** and **29-NH_2** analogues were shown to self-assemble in non-polar solvents. Fluorescence spectra of **29-H** in $CHCl_3$ showed a broad band at 455 nm attributed to "excimer-like" emission caused by face-to-face stacking of aromatic rings in the resulting nanotubular structures. Atomic force microscopy also provided images consistent with formation of tubular stacks, with pore diameters of 2.8 ± 0.2 nm for **29-H** and 2.7 ± 0.2 nm for **29-NH_2**.

Importantly, the authors found that macrocycles **29-H** and **29-NH_2** have different propensities for transporting chloride

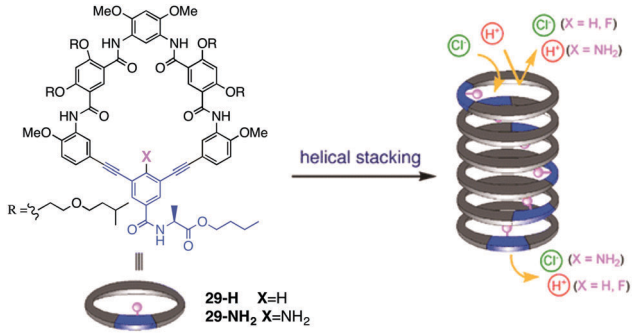

Fig. 5 Structure of oligoamide macrocycles **29-H** and **29-NH$_2$** and self-assembly of monomers into nanotubular pores that conduct ions across lipid membranes. The identity of the –X group on the interior of the pore influences the ion transport selectivity of the self-assembled ion channel. Reproduced from ref. 16. Copyright 2016, American Chemical Society.

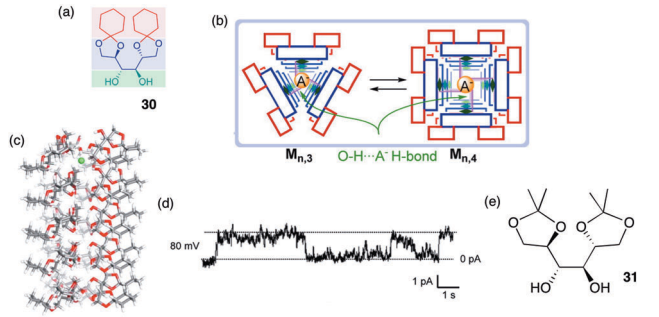

Fig. 6 (a) Structure of mannitol transporter **30**. (b) Schematic of how **30** self-assembles in lipid membrane. (c) Side-view of optimized structure of a 3 × 5 assembly of **30** containing a single Cl^- anion. (d) Single-channel current traces recorded at 80 mV holding potential. (e) Inactive analogue **31**. The main conductance state is indicated by dotted lines. Reproduced from ref. 17. Copyright 2014, American Chemical Society.

across lipid bilayers. They monitored transmembrane chloride transport across vesicles membranes using a Cl^--sensitive dye, *N*-(ethoxycarbonylmethyl)-6-methoxyquinoliniumbromide. This assay revealed that **29-NH$_2$** was a relatively effective Cl^- transporter and the authors proposed that this selectivity was due to the numerous amino groups that would be found on the nanotube's interior, each with a significant partially positive charge that would interact favourably with chloride anions. The authors obtained firm evidence for formation of transmembrane channels by **29-H** and **29-NH$_2$** in a series of single-channel conductance experiments using planar lipid bilayers. Both **29-H** and **29-NH$_2$** showed long-lasting, single conductance states, with respective conductance values of 238 ± 60 and 231 ± 44 pS, values that are entirely consistent with the nm-sized pores.

Most importantly in the context of designing anion-selective channels, the K^+/Cl^- transport selectivity for **29-H** and **29-NH$_2$**, calculated from the ionic flux across a membrane as a function of the transmembrane potential and the concentrations of the ions inside and outside of the vesicle, revealed permeability ratios (P_{K^+}/P_{Cl^-}) of 9 for the **29-H** channel and a reduced value of 3.5 for the **29-NH$_2$** channel. Even though both channels were actually cation-selective, the **29-NH$_2$** channel showed a significant enhancement in its ability to conduct chloride anions across a membrane.

This work by Gong *et al.* has clearly shown how self-assembly of nanotubes with the same outer surface but with different internal functional groups can be used to modulate transport selectively based on charge. Further understanding of the mechanisms that control ion selectively will undoubtedly lead to improved design of future generation transporters that show enhanced transport selectivity for Cl^- and other anions.

An example of a rosette motif in the design of self-assembled anion channels comes from the recent work of Talukdar and colleagues (Fig. 6).[17] These researchers reasoned that the hydroxyl group, which can hydrogen bond with anions, might be useful for designing anion selective channels. The crystal structure of the diketal mannitol **30** showed an infinite chain formed by hydrogen-bonded dimers of **30$_2$**, indicating that this compound has a strong propensity to self-associate in a nonpolar environment. The authors further suggested that stacks of cyclic rosettes formed from 3 or 4 units, **30$_3$** and **30$_4$**, might well provide a transmembrane channel where anions could hop from one layer to the next by forming multivalent O–H···A–hydrogen bonds between adjacent layers.

Indeed, the protected mannitol **30** (m.w. = 342) promoted the transmembrane transport of anions. The authors first used the classical HPTS assay, which monitors the internal pH of a phospholipid liposome, to show that cyclohexylidene **30**, but not an isopropylidene analogue **31** (Fig. 6e), readily dissipates a pH gradient across the DPPC vesicle. The authors attributed the anion transport activity by **30** to a fine balance between hydrophilic interactions, which enable hydrogen-bonding assembly of subunits into a pore, and hydrophobic interactions between the compound's cyclohexyl sidechains and the lipid bilayer, which allows for effective partitioning of **30** into the membrane. Analysis of transport kinetics as a function of transporter concentration revealed an impressive EC_{50} value of 42.5 μM and a Hill coefficient of k = 0.9. This Hill coefficient, which is close to 1, was interpreted to indicate that the active transporter was likely a multimeric assembly that self-associates with a high affinity.

A series of HPTS assays, done as a function of extravesicular anions, showed a halide selectivity of $Cl^- > Br^- > I^-$, which the authors suggested meant that diol **30** preferred to bind Cl^- by forming a series of intermolecular hydrogen bonds. Together the liposomal assays suggested that mannitol derivative **30** is a Cl^- selective anion transporter. These data, however, cannot conclusively determine whether **30** functions as a unimolecular carrier (especially given the Hill coefficient of k = 0.9) or as a self-assembled channel, as might be suggested from the solid-state evidence for self-assembly of **30**. Once again, single channel conductance experiments were used to demonstrate that **30** can function as a self-assembled channel. Distinct single-channel opening and closing events were observed and a single-channel conductance of 38.1 ± 3 pS was determined, which corresponds to a channel diameter of 3.06 Å. This estimate is close to the diameter of a dehydrated Cl^- (d = 3.34 Å). To determine the channel diameter using the Hille equation the length of the

channel formed must be known. In this work, this is estimated to be 34 Å as accurate measurements cannot be made. A small change in the channel's length could account for the 10% discrepancy between the two estimated values. Molecular models of a channel based on stacks of cyclic trimers showed a diameter of 3.23 Å, which agreed with the channel diameter of 3.06 Å obtained from the single-channel conductance measurements. Molecular dynamics calculations on a trimeric channel embedded in a slab of DPPC membrane also supported a hopping mechanism for Cl^- transport; the anion makes and breaks O–H···Cl^- hydrogen bonds as it moves through the channel *via* a relay mechanism, being passed along from one trimeric rosette to the next layer of –OH groups.

More recently, Talukdar's group has again demonstrated that a small molecule, this time the bis-diol **32** shown in Fig. 7, can be used for the self-assembly of a synthetic anion channel.[18] Formation of the active structure is proposed to be due to intermolecular hydrogen bonds between the –OH hydroxyl groups on neighboring molecules. Anion transport activity, which was again determined using the HPTS base-pulse fluoresence assay, showed that the identity of the alkyl chains on the amine group of **32** was important for Cl^-/OH^- exchange, as efficient rates of anion transport required an optimal log *P* values. Single-channel conductance experiments in planar bilayers clearly showed that **32** formed ion channels in DPhPC membranes, as depicted in Fig. 7c. Energy-minimized models of the self-assembled channel of $\mathbf{32}_n$ showed a nanotube lined with hydroxyl groups that point toward the nanotube's cavity and are well oriented for binding and transporting Cl^- anion. In this paper, the authors also carried out extensive biological studies using bis-diol **32**. They found that **32** could transport Cl^- into cells and also trigger cell death in a number of different cell lines. Furthermore, a battery of experiments using various dye-based assays and confocal microscopy showed that Cl^- transport catalyzed by bis-diol **32** disturbed the electrical potential across mitochondrial membranes, which subsequently led to generation of reactive oxygen species and triggered release of cytochrome *c* from the mitochondria. The authors concluded that this type of cell death caused by **32** was due to apoptosis, as was supported by the over-expression of caspase proteins upon treatment of cells with bis-diol **32**. The ability of small molecule such as bis-diol **32** to induce apoptosis, presumably *via* a chloride transport process, may have therapeutic potential in treatments of various diseases.

Vargas Jentzch and Matile reported that rigid-rod scaffolds outfitted with tetrafluoroiodobenzyl sidechains catalyzed the transmembrane transport of Cl^- and NO_3^- anions[19] although they did not explicitly claim formation of transmembrane channels. Octamer **33**, whose length approaches that of the hydrophobic bilayer, was the most active transporter in the series. The authors attributed the anion transport activity to the ability of these oligomers to provide a "hopping" pathway, whereby the anions can bind reversibly using both anion–π interactions and also halogen bonds with the σ-holes of the iodine atoms (Fig. 8). Matile's group had previously shown that halogen bonds in small molecules, such as pentafluoroiodobenzene or a calix[4]arene with four halogen-bond donors, could help transport anions, albeit relatively inefficiently, across membranes. The authors reasoned that anions likely bind to the pentafluoroiodobenzene monomer too weakly to allow for efficient transport; and anions bind too strongly to the convergent donors on the calix[4]arene macrocycle to allow high transport rates. To address this problem the authors used linear *p*-oligophenyl oligomers, compounds that can presumably self-assemble and span the hydrophobic membrane, so as to provide a kinetically feasible pathway for chloride anions to hop from one binding site to another as they move across the membrane.

The authors used the classical HPTS assay to monitor Cl^-/OH^- exchange across large unilamellar vesicles (LUVs) made

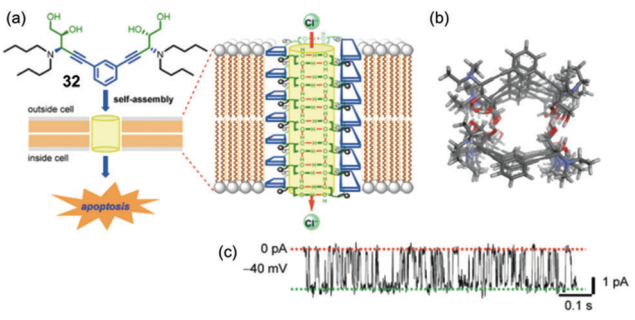

Fig. 7 (a) Schematic depicting of a self-assembly of bis-diol **32** in a lipid membrane. The Cl^- selective channel that spans the membrane is proposed to consist of stacks of hydrogen bonded dimers of $\mathbf{32}_2$. Transmembrane transport of chloride anions, which triggers apoptosis in a number of tested cell lines, is mediated by O–H···Cl^- hydrogen bonds. (b) Top view of optimized structure of the anion channel formed by self-assembly of bis-diol **32**. (c) Single-channel current traces recorded at −40 mV holding potential in 1 M symmetrical KCl solution. The main conductance state is indicated by dotted lines. Reproduced from ref. 18. Copyright 2016, American Chemical Society.

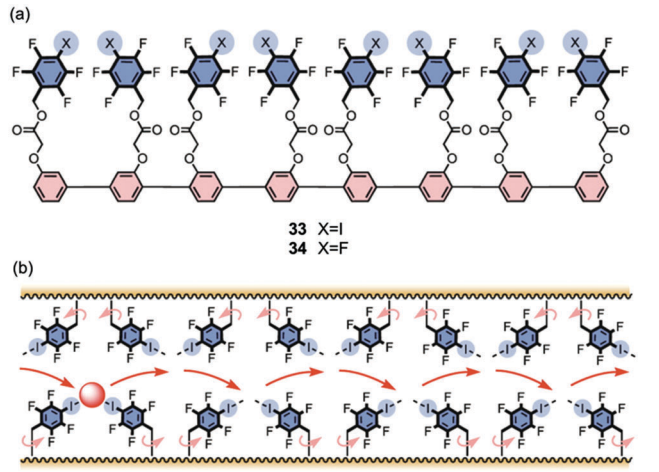

Fig. 8 (a) Structures of rigid-rod transporters **33** and **34**. Octamer **33**, the most active transporter studied, is proposed to use both anion–π and halogen bond interactions to facilitate membrane transport of anions. (b) Schematic representation of how halogen bonding enables hopping of the anion from one binding site to the next as it moves through the lipid membrane. Reproduced from ref. 19. Copyright 2013, American Chemical Society.

from egg yolk phosphatidylcholine (EYPC). Compounds such as **33** that contain the halogen-bonding motif, tetrafluoroiodo side-chains, were better anion transporters (by 3.5–26 fold) than those with pentafluorobenzyl groups, such as **34**, which could only provide anion–π interactions. Importantly, the activity of both the anion–π and the halogen-bond transporters increased with length, reaching a maximum when the rods were the right length to span the hydrophobic section of the bilayer. Thus, the octamer transporter **33** showed an EC_{50} value of just 100 nM and had an impressive cooperativity coefficient of $m = 3.37$, making it 2360 times more active than monomeric pentafluoroiodobenzene. This study demonstrated that compounds that combine the attractive characteristics of the rigid-rod backbone with appendages providing transient anion binding sites using anion–π interactions and halogen bonds are quite impressive anion transporters. Presumably these compounds self-assemble to give bundles that help anions skip across the membrane.

One example of an unimolecular channel that conducts Cl^- anions was recently described by Hou, Li and colleagues.[20] They reported that relatively low concentrations (EC_{50} = 0.002 mol%) of pillar[*n*]arenes (*n* = 5, 6) with multiple peptide side-chains attached to the central core were able to transport amino acids across EYPC vesicles and do so enantioselectively for certain amino acids. They proposed that these compounds, which contained repeats of the non-polar phenylalanine in the peptide arms, folded into unimolecular channels within the bilayer membranes. A series of ^1H NMR experiments in CD_2Cl_2 revealed that the peptide chains of **35** formed strong intramolecular hydrogen-bonds in this non-polar solvent. Similarly, infrared studies of these compounds embedded in EYPC vesicles also supported formation of an intramolecular hydrogen-bonded fold within the membrane. Energy-minimized models showed that these pillar[*n*]arenes formed a tubular structure, suggestive of a channel. While the paper's focus was on the unique ability of these pillar[*n*]arenes to transport amino acids across membranes, the authors noted that some natural amino acid transporters are also able to transport chloride anions across cell membranes. Indeed, by using the Cl^- sensitive dye lucigenin Hou and colleagues demonstrated that compounds **35** and **36** also catalyzed transmembrane Cl^- transport across EYPC membranes. Although more studies need to be done to confirm channel activity and determine anion selectivity, this interesting result demonstrates that the pillarene motif could be quite useful for building unimolecular anion channels (Fig. 9).

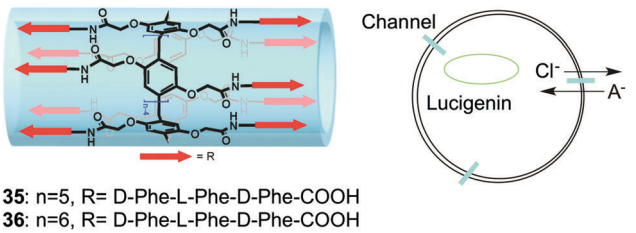

Fig. 9 Schematic representations of pillararene transporters **35** and **36** (left) and representation of transmembrane Cl-transport mediated by compounds **35** and **36**. Adapted from ref. 20. Copyright 2013, American Chemical Society.

Optimising transport

The development of efficient anion transporters (*i.e.* compounds that have low EC_{50} values or high initial chloride efflux rates and hence can be used in low concentration) has attracted much interest and effort over recent years. By drawing an analogy to drug delivery and medicinal chemistry a number of research groups have made the link between the efficiency of a transporter and its lipophilicity. This is illustrated by Quesada and co-workers' study of the role of lipophilicity in anion transport processes mediated by tambjamines (Fig. 10).[21] The chloride/bicarbonate antiport properties of tambjamines **37–52**, that span a wide range of log *P* values (*n*-octanol/water partition coefficient), were studied in POPC vesicles (Fig. 11) using a chloride selective electrode to monitor chloride flux from the vesicles. Separate experiments using ^{13}C labelled HCO_3^- were used to confirm directly bicarbonate transport. The initial rate of chloride transport in the ion selective electrode experiments was plotted against calculated log *P* (Fig. 12) showing a parabolic relationship between log *P* and initial chloride transport rate and an optimum log *P* for transport of around 4.2. The authors hypothesise that the compounds with lower log *P*s are too hydrophilic to partition effectively into the lipid bilayer than compounds with optimal log *P* values. The lower activity of the compounds with higher log *P* values was attributed to poorer deliverability of these compounds from the aqueous phase to the lipid bilayer and/or lower mobility of these tambjamines within the lipid bilayer. This relationship is very well known to medicinal chemists in

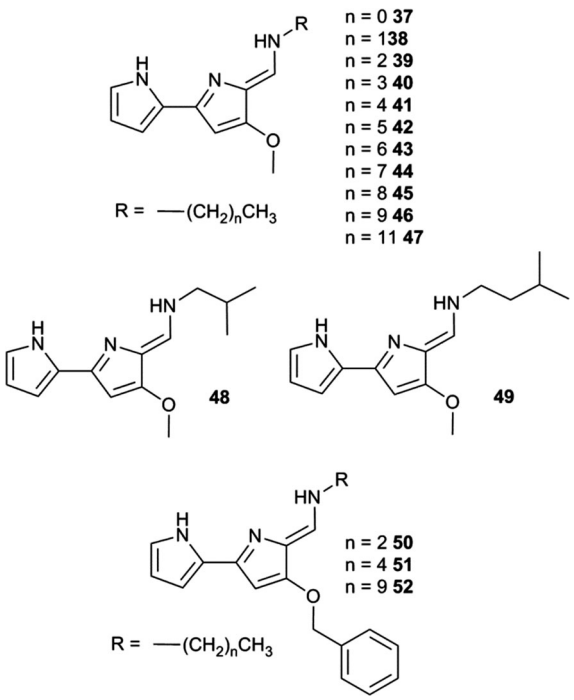

Fig. 10 Tambjamine derivatives **37–52**.

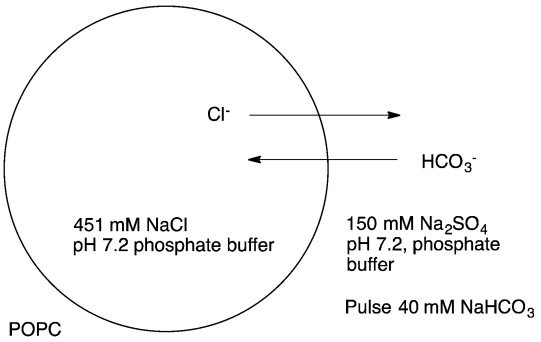

Fig. 11 Anion transport experiments with compounds **37–52**.

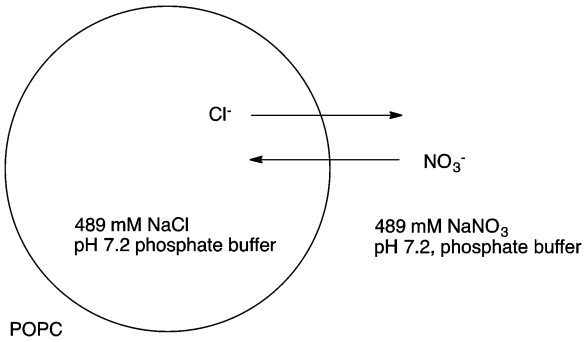

Fig. 14 Anion transport experiments with compounds **53–74**.

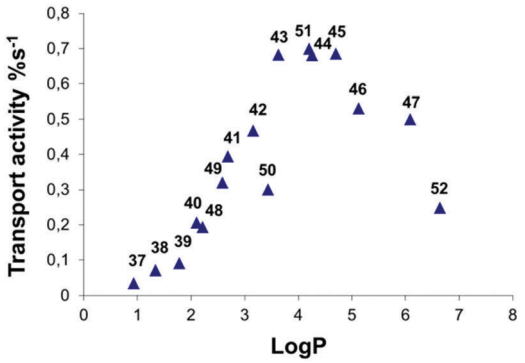

Fig. 12 Representation of transport activity, measured as initial chloride efflux ($\%s^{-1}$) *vs.* calculated average log *P* for compounds **37–52**.

which the activity of a drug has an optimal value and a parabolic relationship with log *P*.

Gale and co-workers synthesized an extended series of 1-hexyl-3-phenylthioureas **53–74** with a variety of substituents on the 4-position of the phenyl ring (Fig. 13).[22] These substituents were chosen to have a range of lipophilicities and electron withdrawing or electron donating effects. A Hill analysis was conducted with each of the transporters giving an EC_{50} for chloride/nitrate exchange (Fig. 14). A quantitative structure–activity relationship study was performed using Hansch analysis to determine the

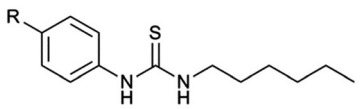

53	R = Br	**64**	R = O(CO)Me
54	R = CF_3	**65**	R = OCF_3
55	R = Cl	**66**	R = OEt
56	R = CN	**67**	R = OMe
57	R = $COCF_3$	**68**	R = SMe
58	R = COMe	**69**	R = SO_2Me
59	R = COOMe	**70**	R = CH_3
60	R = F	**71**	R = CH_2CH_3
61	R = H	**72**	R = $(CH_2)_2CH_3$
62	R = I	**73**	R = $(CH_2)_3CH_3$
63	R = NO_2	**74**	R = $(CH_2)_4CH_3$

Fig. 13 1-Hexyl-3-phenylthioureas **53–74**.

molecular parameters that are key in determining how a receptor will perform as an anion transporter.

The analysis resulted in eqn (1) and (2) being obtained. The first term in each equation relates to lipophilicity (retention time, RT or log *P*) and has a positive effect of transport. Retention time on a reverse phase HPLC column is related to the lipophilicity of the compound. So in this set of compounds an increase in lipophilicity results in increased anion transport ability. The second term in both equations is the Hammett coefficient of the substituent on the 4-position of the phenyl ring. The positive sign of this term means that as the Hammett coefficient increases so the affinity of the thiourea for anionic guests increases as does its anion transport ability. The next term SPAN is related to the size of the molecule. This term is presumably related to diffusion of the transporter through the membrane with the negative sign meaning that as the molecule gets bigger its transport ability decreases. The relative importance of each term is shown graphically in Fig. 15 which highlights the dominance of lipophilicity in determining anion transport ability.

$$\log(1/EC_{50}) = 0.94(\pm0.07) \times RT + 0.48(\pm0.14) \times \sigma_p - 0.31(\pm0.07) \times \text{SPAN} - 9.0(\pm0.8)$$
$$N = 18,\ R^2 = 0.93,\ R_{adj}{}^2 = 0.92,\ \text{RMSE} = 0.17,\ F = 68 \quad (1)$$

$$\log(1/EC_{50}) = 0.81(\pm0.08) \times \log P + 0.65(\pm0.19) \times \sigma_p - 0.29(\pm0.09) \times \text{SPAN} - 0.73(\pm0.79)$$
$$N = 18,\ R^2 = 0.89,\ R_{adj}{}^2 = 0.87,\ \text{RMSE} = 0.21,\ F = 39 \quad (2)$$

More recently, Spooner and Gale have investigated a set of similar thioureas **75–89** (Fig. 16) with a wider range of lipophilicities (Table 1) in lipid bilayers consisting of a number of different lipids (Fig. 17).[23] The chloride/nitrate antiport properties of these compounds were measured under the conditions shown in Fig. 14 in a variety of different lipids and mixtures of lipids including POPC, POPG, and 3 : 1 POPE : POPC. The initial rate of chloride transport was plotted against clog *P* (Fig. 18) and it was found that under the three sets of conditions whilst the initial rate would vary the optimal log *P* for transport remained constant.

Following on from Gale's work on tren-based tripodal ureas and thioureas,[24] this group decided to prepare very simple

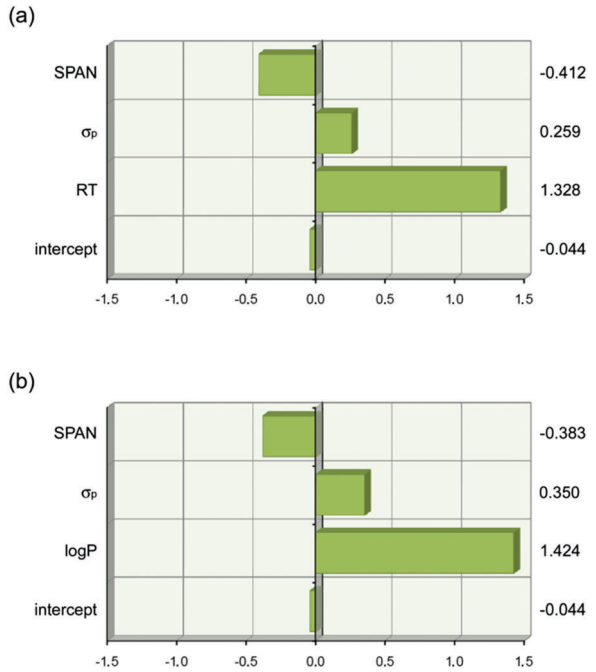

Fig. 15 Graphical depiction of the values of the coefficients in eqn (1) and (2) when the descriptor values are scaled to have a mean of zero and a range of two using JMP 9.0.0. This shows that lipophilicity (RT or log *P*) has the strongest effect on anion transport. The values of the scaled coefficients for each descriptor are shown on the right hand side. (a) Eqn (1). (b) Eqn (2).

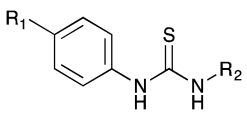

Fig. 16 The general structure of the thioureas studied by Spooner and Gale.

Table 1 Calculated log *P* values for compounds **75–89**

Cmpd	R_1	R_2	clog *P*	Cmpd	R_1	R_2	clog *P*
75	H	Et	2.19	**83**	Pe	Pe	5.94
76	Me	Et	2.68	**84**	Pe	Hx	6.40
77	Et	Et	3.14	**85**	Hx	Hx	6.85
78	Et	Pr	3.66	**86**	Hx	Hp	7.31
79	Pr	Pr	4.12	**87**	Hp	Hp	7.77
80	Pr	Bu	4.57	**88**	Hp	Oc	8.22
81	Bu	Bu	5.03	**89**	Oc	Oc	8.68
82	Bu	Pe	5.49				

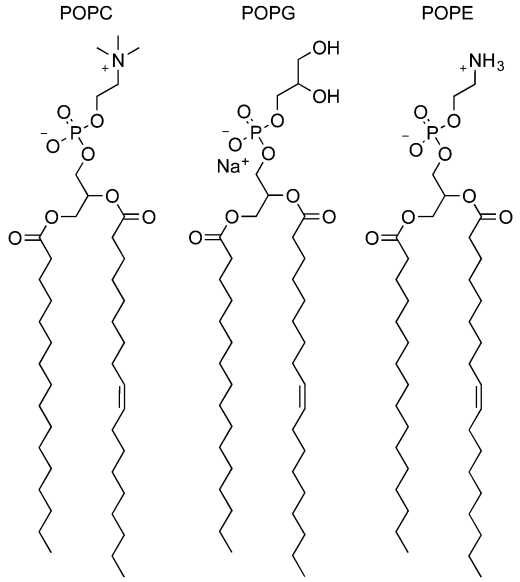

Fig. 17 Structures of 1-palmitoyl-2-oleoyl-*sn*-*glycero*-3-phosphocholine (POPC), 1-palmitoyl-2-oleoyl-*sn*-*glycero*-3-phosphoglycerol (POPG) and 1-palmitoyl-2-oleoyl-*sn*-*glycero*-3-phosphoethanolamine (POPE).

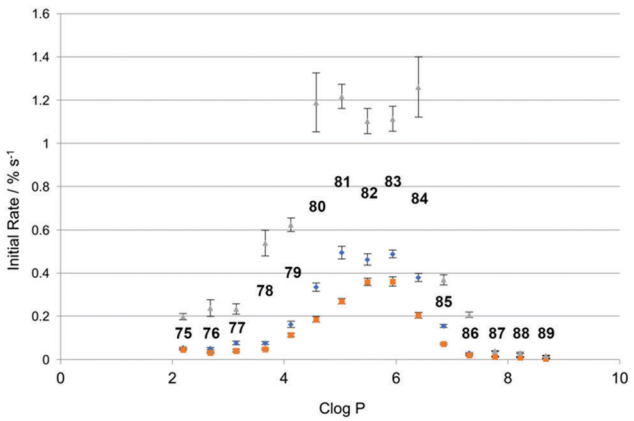

Fig. 18 Plot of initial rate of chloride efflux from various lipid vesicles (containing 489 mM NaCl buffered to pH 7.2 with 5 mM sodium phosphate salts) for **75–89** (1% loading w.r.t. lipid), plotted against clog *P* of the transporter molecule. Vesicles suspended in 489 mM $NaNO_3$, buffered to pH 7.2 with 5 mM sodium phosphate salts. Blue diamonds: 100% POPC; orange squares: 100% POPG; grey triangles: 3 : 1 POPE : POPC. Each point represents the average of 3 trials. Error bars represent the standard error on the linear regression.

compounds containing a single urea or thiourea group and assess the ability of these systems to mediate chloride/nitrate and chloride/bicarbonate antiport (Fig. 19).[25] Smaller molecules may obey 'Lipinski's rule of 5' and hence are more likely to have acceptable ADME (absorption, distribution, metabolism and excretion) properties. Transport experiments were run under the conditions shown in Fig. 14 for chloride/nitrate exchange and by the bicarbonate pulse method discussed above for chloride/bicarbonate. Carbon-13 NMR experiments with $H^{13}CO_3^-$ were used to confirm directly bicarbonate transport. The set of ureas proved ineffective at mediating both chloride/nitrate and chloride/bicarbonate exchange. However, the more lipophilic thioureas were effective at mediating both processes with the lowest EC_{50} values observed with compound **95** (Table 2). Compound **95**, which combines a higher clog *P* and lower polar surface area than its inactive urea analogue, proved to be a remarkably potent anion transporter functioning in concentrations as low as 1 : 25 000 carrier to lipid ratio for chloride/nitrate exchange.

Previous work by Gale had shown that fluorinated tren-based transporters were more effective than their parent analogues.[26] Therefore series of fluorinated and non-fluorinated indole ureas and thioureas **96–99** were synthesised and their anion transport properties compared. The binding mode of compound **98** with

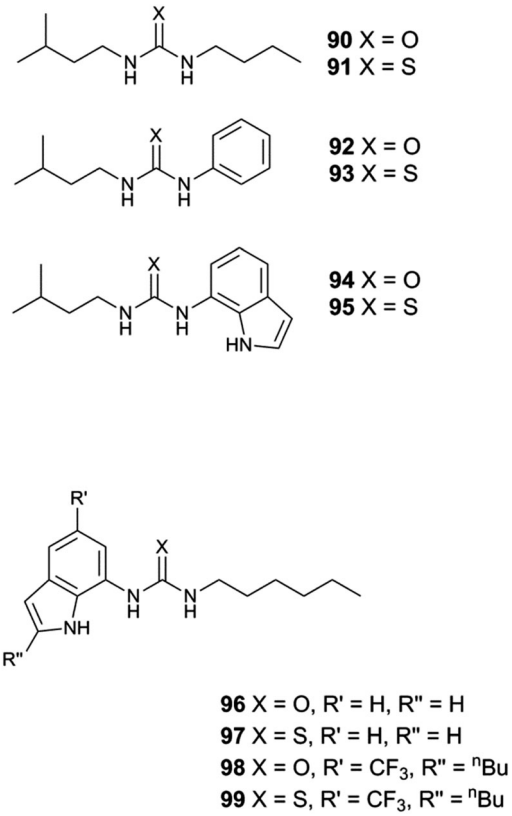

Fig. 19 Indole urea and thiourea-based receptors **90–99**.

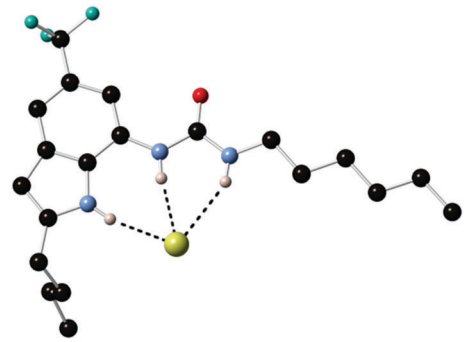

Fig. 20 X-ray crystal structure of the chloride complex of **98**. Non-acidic hydrogens and counter cation have been omitted for clarity.

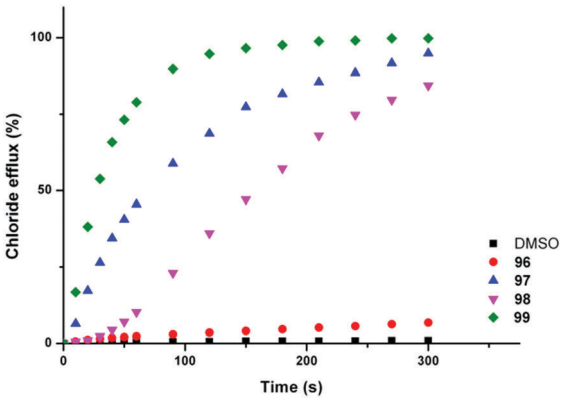

Fig. 21 Chloride efflux promoted by a DMSO solution of compounds **96–99** (2 mol% carrier to lipid) from unilamellar POPC vesicles loaded with 489 mM NaCl buffered to pH 7.2 with 5 mM sodium phosphate salts. The vesicles were dispersed in 489 mM $NaNO_3$ buffered to pH 7.2 with 5 mM sodium phosphate salts. At the end of the experiment, detergent was added to lyse the vesicles and calibrate the ISE to 100% chloride efflux. Each point represents an average of three trials. DMSO was used as a control.

chloride was revealed in the X-ray crystal structure of the tetrabutylammonium chloride salt of this receptor (Fig. 20). Compound **98** forms three N–H hydrogen bonds with the chloride ion (N–Cl distances 3.140(5)–3.406(5) Å, N–H···Cl angles 151.2–170.1°).

Chloride/nitrate antiport was demonstrated in a series of experiments with the fluorinated systems showing enhanced transport abilities as compared to the non-fluorinated analogues (Fig. 21 and Table 3). Presumably this enhancement is due in part to the enhanced lipophilicity of the derivatives with trifluoromethyl-substituents (Table 3). Similar results were obtained for chloride/bicarbonate exchange. Cell studies showed that the fluorinated compounds could de-acidify acidic organelles within melanoma (A375) cells and could reduce the viability of a range of human cancer cell lines in particular GLC4 (small cell human lung cancer) whilst the non-fluorinated compounds only had a limited effect on cell viability.

Table 2 EC_{50} (270 s) values and initial rate of chloride release (% chloride efflux per second) for compounds **91**, **93** and **95** for release of chloride in chloride/nitrate and chloride/bicarbonate systems. Calculated log *P* and TPSA (Å^2) are also presented for compounds **90–95**

Compounds	EC_{50} at 270 s (Cl^-/NO_3^-)	Initial rate of chloride release (Cl^-/NO_3^-)% Cl^- efflux/s at 2% carrier loading	EC_{50} at 270 s (Cl^-/HCO_3^-)	Initial rate of chloride release (Cl^-/HCO_3^-)% Cl^- efflux/s at 2% carrier loading	clog *P*[a]	PSA[b] (Å^2)
90	—	—	—	—	1.99	37.0
91	0.1491%	0.431	0.6049%	0.227	3.14	22.2
92	—	—	—	—	2.42	34.8
93	3.0667%	0.074	2.7848%	0.188	3.57	21.5
94	—	—	—	—	2.02	44.6–47.7
95	0.02663%	0.614	0.0405%	0.386	3.16	31.3–35.5

[a] clog *P* calculated using Spartan '08 for Macintosh (Ghose–Crippen model). [b] Polar surface area (PSA) calculated using Spartan '08 for Macintosh. The receptors were minimised using AM1 semi-empirical methods with the two urea or thiourea NH groups parallel and the PSA and log *P* values calculated. In the case of the case of the indole containing species two conformations were minimised – one with the indole NH forming a convergent array with the urea NH groups and the other with the indole NH oriented towards the urea or thiourea O or S atom (hence a range of values for PSA are given).

Table 3 Overview of transport assays and lipophilicity of compounds **96–99**

	clog P^a	$EC_{50,270s}{}^b$ (Cl^-/NO_3^-)	n^c (Cl^-/NO_3^-)	$EC_{50,270s}{}^b$ (Cl^-/HCO_3^-)	n^c (Cl^-/HCO_3^-)
96	3.87	[d]	[d]	[d]	[d]
97	4.03	0.029	0.8	0.18	0.7
98	6.23	0.47	1.3	1.2	2.0
99	6.40	0.016[e]	1.7[e]	0.081[e]	1.5[e]

[a] clog P calculated using Fieldview 2.0.2 for Macintosh (Wildman–Crippen model). [b] $EC_{50,270s}$ defined as concentration (mol% carrier with respect to lipid) needed to obtain 50% efflux after 270 s. [c] Hill coefficient. [d] Accurate Hill analysis could not be performed due to low activity. [e] Some of the observed activity is from H^+/Cl^- co-transport.

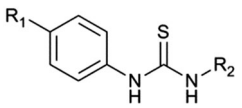

100a R_1 = H, R_2 = hexyl
100b R_1 = ethyl, R_2 = hexyl
100c R_1 = H, R_2 = undecyl
100d R_1 = ethyl, R_2 = nonyl
100e R_1 = pentyl, R_2 = hexyl
100f R_1 = octyl, R_2 = propyl
100g R_1 = nonyl, R_2 = ethyl
100h R_1 = penyl, R_2 = cyclohexyl

Fig. 22 Compounds **100a–100h**.

A. P. Davis, Gale and co-workers investigated how the structure of a series of thioureas with similar log P values affects their transport properties.[27] In order to do this it was necessary to find transporters that resided solely within the lipid bilayer membrane and were not partitioned between the aqueous and lipid phases (Fig. 22). A preliminary study of compounds **100a**, **100b** and **100e** (R_2 = C_6H_{13}; R_1 = H, C_2H_5, C_5H_{11}; C_{total} 6, 8 and 11 respectively) was conducted using lucigenin containing POPC/cholesterol vesicles with the transporter present in the membrane. The vesicles contain sodium nitrate and are suspended in sodium chloride solution. Transport experiments were conducted with suspensions of vesicles at 0.4 mM, 0.2 mM and 0.1 mM lipid concentration. If the transporter is partitioned between the two phases, its activity will depend on lipid concentration. However if it is residing within the lipid bilayer solely then transport activity should be independent of concentration. It was found that this was true for compound **100e** and so a total of 11 aliphatic carbons on the thiourea were necessary to confine the transporter to the lipid bilayer. A transport study was then conducted on compounds **100c**, **100d**, **100e**, **100f** and **100g** which all contain 11 aliphatic carbons. It was found that compound **100e** had the highest transport activity with the activities of the other compounds falling off as the thiourea group gets closer to either end of the molecule. The authors refer to this effect as lipophilic balance and attribute it to the extra stability of the transporter–chloride complexes in which the thiourea is at the end of the molecule essentially forming an amphiphile that is more stable at the lipid:water interface than complexes in which the anion binding site is in the centre of the molecule.

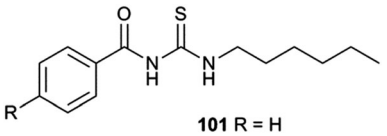

101 R = H
102 R = CF_3
103 R = OMe
104 R = n-pentyl

Fig. 23 The structures of acylthioureas **101–104**.

Gale and co-workers have synthesised a series of acylthioureas **101–104** (Fig. 23) and studied the anion transport ability of these compounds.[28] In the absence of an anionic guest these compounds may form an intramolecular hydrogen bond (Fig. 24) which may affect their ability to transport anions. The anion transport properties of parent compound **101** were compared with thiourea analogue **100a** in a chloride/nitrate antiport study (Fig. 25). The acylthiourea was found to have significantly enhanced transport properties compared its thiourea analogue (Table 4) with HPLC retention time experiments on a C18 reverse phase column revealing the enhanced lipophilicity of these compounds compared to their thiourea analogues. The authors attribute this enhancement to a lower propensity of the intramolecularly hydrogen bonded compounds to interact with water.

A. P. Davis and co-workers have used lipophilic scaffolds such as cholic acid to construct very effective anion transporters.

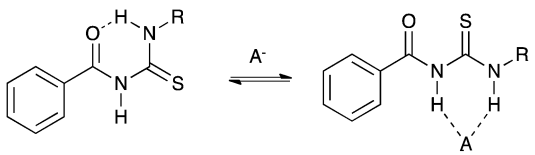

Fig. 24 Competition between intramolecular hydrogen bond formation and anion binding in acylthiourea receptors.

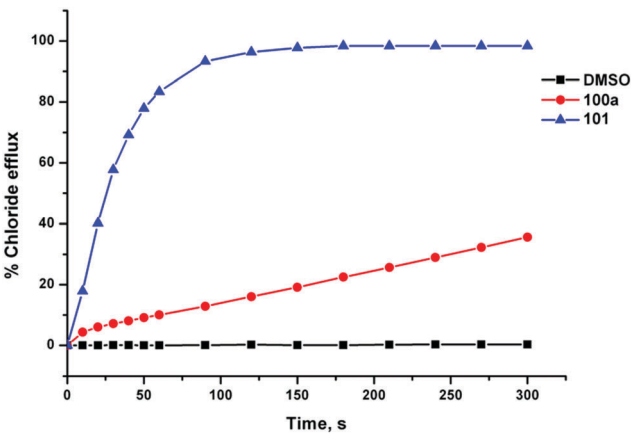

Fig. 25 Chloride efflux mediated by unsubstituted receptors **100a** and **101** (2 mol% with respect to lipid) from unilamellar POPC vesicles containing 489 mM NaCl buffered to pH 7.2 with 5 mM sodium phosphate salts. The vesicles were suspended in 489 mM $NaNO_3$ buffered to pH 7.2 with 5 mM sodium phosphate salts. At the end of the experiment the vesicles were lysed with detergent in order to calibrate 100% chloride release. Each point represents the average of three trials.

Table 4 Retention times (determined by reverse phase C18 HPLC experiment) and transport data (determined by Hill plot) for compounds **100a–104**. EC_{50} is defined as the concentration (mol% with respect to lipid) of receptor required to mediate 50% chloride efflux after 270 s; *n* is the Hill coefficient

Receptor	Retention time/min	Cl^-/NO_3^- [a] EC_{50}	Error	*n*	Cl^-/HCO_3^- [b] EC_{50}	Error	*n*
100a	4.9	2.7	±0.6	0.90	3.1	±0.10	±0.6
101	8.9	0.33	±0.06	2.07	0.27	±0.27	±0.78
102	10.5	0.69	±0.01	2.76	8.1	±0.24	±0.77
103	9.4	0.28	±0.02	2.03	0.28	±0.11	±0.91
104	12.9	1.1[c]	±0.1[c]	2.3[c]	6.5[c]	±0.21[c]	±1.5[c]

[a] Transport data is the average of a minimum of 3 repeated Hill plot experiments. The error given is the standard deviation. [b] Transport data is the result of a single Hill plot analysis (therefore no errors are given). [c] Activity dependent on stock concentration of receptor solution-data gathered using only a 5 mM solution.

Recently this group has expanded the palette of scaffolds available with reports of the use of *trans*-decalins[29] and cyclohexane.[30]

Transdecalins appended with two urea groups **105a–105i** (Fig. 26) were prepared and their anion transport properties studied by chloride transport into vesicles containing $NaNO_3$ (225 mM) and lucigenin.[29] The results revealed that compound **105i** (presumably the most lipophilic) was the most powerful transporter from this series and the data compared to cholapod **106** (Fig. 27). Compound **105i** was shown to function in transporter to lipid ratios as low as 1 : 250 000 (Fig. 27c).

A. P. Davis and co-workers have also developed families of transporters using a cyclohexane scaffold.[30] Two families were prepared (**107** and **108** – Fig. 28). Both families consist of a

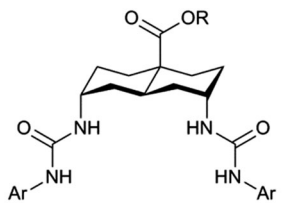

105a R = Me, Ar = Ph
105b R = Me, Ar = 4-CF_3-C_6H_4-
105c R = Me, Ar = 3,5-bis-$CF_3C_6H_3$-
105d R = Et, Ar = Ph
105e R = Et, Ar = 4-CF_3-C_6H_4-
105f R = Et, Ar = 3,5-bis-$CF_3C_6H_3$-
105g R = Octyl, Ar = Ph
105h R = Octyl, Ar = 4-CF_3-C_6H_4-
105i R = Octyl, Ar = 3,5-bis-$CF_3C_6H_3$-

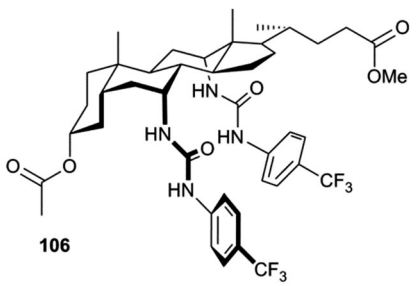

106

Fig. 26 The structures of diureido-decalins **105a–105i** and cholapod **106**.

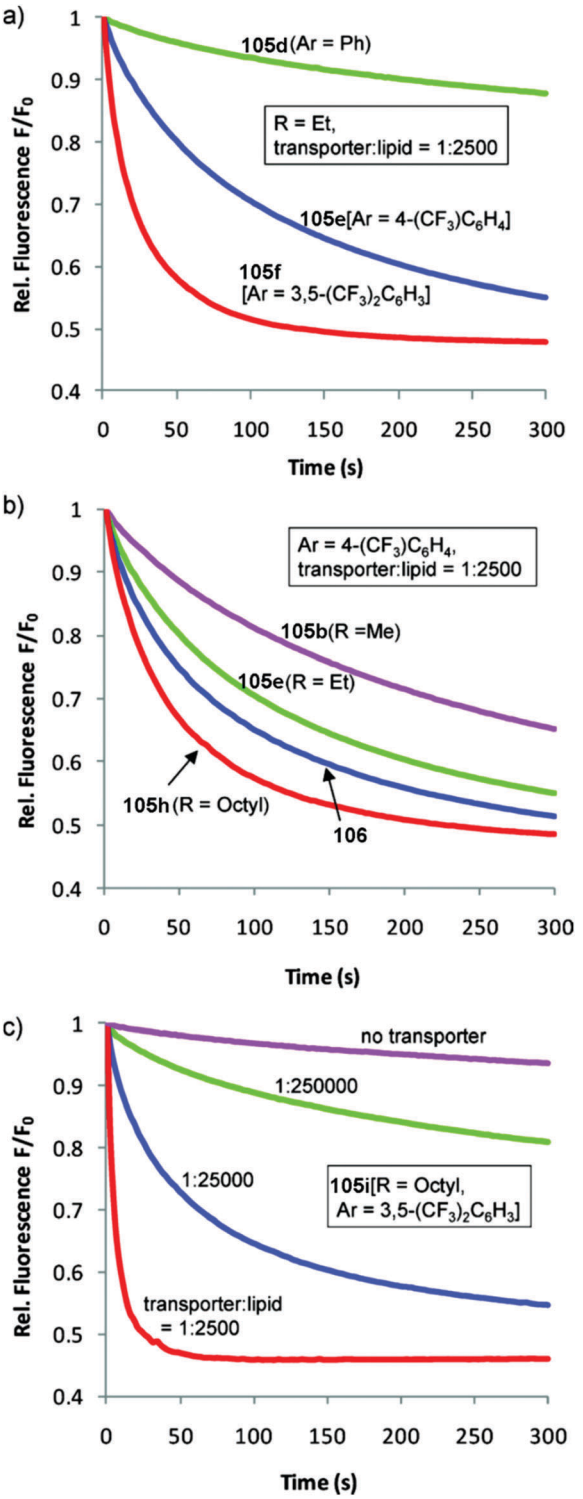

Fig. 27 Chloride transport by decalins **105a–i** into vesicles containing $NaNO_3$ (225 mM) and lucigenin: (a) varying Ar (R = Et, transporter/lipid = 1 : 2500); (b) varying R (Ar = 4-trifluoromethylphenyl, transporter/lipid = 1 : 2500). Data for cholapod **106** are also shown. (c) Varying the transporter : lipid ratio for **105i**, the most powerful of the transporters studied. Reproduced from ref. 29. Copyright 2011, American Chemical Society.

cyclohexane ring that has three urea or thiourea groups in axial positions linked by a methylene spacer. In **108** each spacer is

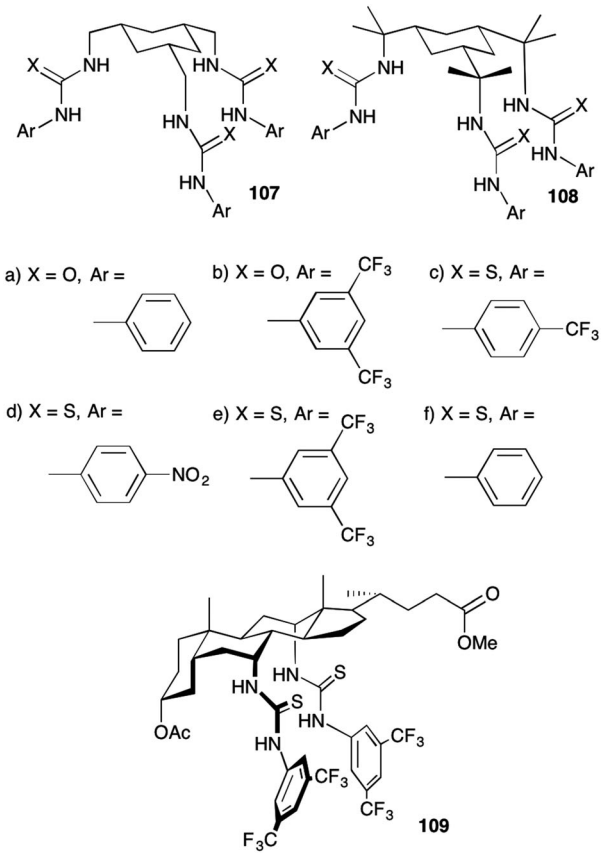

Fig. 28 The structures of families of compounds based on cyclohexane **107** and **108** and cholapod **109**.

functionalised with two methyl groups which act to favour the axial/in arrangement of the urea/thiourea groups and also compress the binding site so shortening potential hydrogen bonding interactions to within optimal ranges from crystallography. Proton NMR titration methods in DMSO-d_6/0.5% water were used to determine the affinity of these compounds for chloride. The results (Table 5) show moderate affinities with the methylated series **108** having higher affinities than the unmethylated compounds **107**. Chloride/nitrate exchange using the same lucigenin method was employed to study the transdecalin systems and the results compared against those obtained for cholapod **109**. It was found that the most active compound from the cyclohexanes, compound **108e**, is three times more active than cholapod **109** despite the compounds having similar sizes and calculated log *P* values (and compound **108e** having significantly lower affinity for chloride) and is amongst the most active compounds synthesised in Davis's group (with transport easily detectable at 1 : 500 000 carrier to lipid concentrations). The authors attribute the effectiveness of this series of compounds to the increased flexibility which whilst lowering anion affinity accelerates binding kinetics.

Another simple scaffold – a single phenyl ring – has been employed by Gale and co-workers to prepare a variety of 1,2-bisurea compounds which are particularly effective anion transporters[31] and are discussed below in terms of their biological activity.

Table 5 Chloride binding affinities (K_a, M^{-1}) and transport data (chloride/nitrate exchange transporter : lipid 1 : 2500)[b] for the families of compounds **107** and **108** based on cyclohexane

Compound	K_a[a] (M^{-1})	I[c] [s^{-1}]	$t_{1/2}$[d] [s]
107a	27	[e]	[e]
107b	57	[f]	[f]
107c	68	0.00091	440
107d	79	0.0014	340
107e	99	0.0046	120
108a	180	[e]	[e]
108b	390	0.036	16
108c	400	0.029	22
108d	480	0.01	66
108e	670	0.065	9
108f	340	0.0017	190
109	12 000	0.093	6

[a] To *n*-$Bu_4N^+Cl^-$ in DMSO-d_6/0.5% water measured by ^1H NMR titration. T = 298 K. [b] In 200 nm vesicles formed from POPC/cholesterol (7 : 3) measured by following the decay of lucigenin fluorescence F. [c] Initial rate of relative fluorescence change, F/F_0. [d] Decay half-life of F/F_0. [e] Not measured due to low solubility. [f] Fluorescence decay indistinguishable from background.

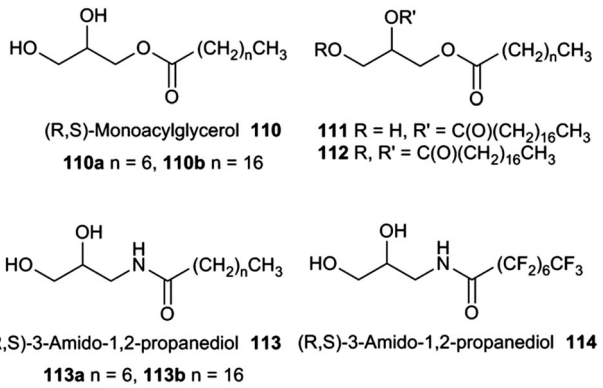

Fig. 29 The structures of compounds **110** to **114**.

J. T. Davis and co-workers have shown that the natural product monoacylglycerol **110a** functions as a chloride/nitrate anion antiporter (Fig. 29).[32] The group first looked at substitution of glycerol unit and found that in lucigenin chloride/nitrate exchange in egg-yolk phosphatidylcholine (EYPC) vesicles compound **110b** promoted chloride influx whilst compounds **111** and **112** proved to be inactive so demonstrating that the 1,2-diol unit is needed for transport. The group then designed compounds **113a** and **114** that may have augmented anion binding transport properties compared to parent compound **110a.** These compounds contain an additional hydrogen bond donor and in the case of **114** a fluorinated chain both of which are expected to enhance the compounds' anion transport properties based on previous studies. The results (Table 6) show that the fluorinated compound **114** is almost 20 times better at facilitating chloride/nitrate antiport than parent compound **110a.**

Method development

Plavec, Jolliffe, Gale and co-workers have developed a new NMR assay for sulfate transport.[33] Sulfate is often used in anion

Table 6 Chloride binding constants, EC_{50} values, Hill coefficients (n) for chloride transport and log P values for monoacylglycerol analogues **110a**, **113a** and **114**

	Ester **110a**	Amide **113a**[a]	Perfluoro **114**
K_a (M^{-1}) $CDCl_3$	92 ± 1.7	1474 ± 32	—
K_a (M^{-1}) CD_3CN	—	137 ± 1.8	193 ± 7.6
EC_{50} 270 s (mM)	0.195 ± 0.01	0.078 ± 0.002	0.011 ± 0.002
Hill coefficient	1.45 ± 0.17	1.12 ± 0.045	0.83 ± 0.20
clog P	1.64	0.97	2.99

[a] Hill analysis of the C18 amide **113a** showed that the length of the acyl chain in **113a** (C8) *vs.* **113b** (C18) had little influence on the transport efficiency, as **113b** had an EC_{50} value of 0.076 ± 0.004.

transport experiments as its high energy of hydration (ΔG_{hyd} = −1080 kJ mol^{-1}) was believed to prevent the anion being transported from an aqueous phase into a lipid bilayer. Commonly in bicarbonate/chloride exchange experiments vesicles containing sodium chloride would be suspended in sodium sulfate solution and a pulse of sodium bicarbonate added in the extra-vesicular solution to initiate chloride/bicarbonate exchange. Prior to the addition of bicarbonate no chloride transport should be observed in the presence of a transporter, as sulfate back transport would not occur to balance the charge gradient created by chloride efflux. It was during a series of these experiments with tren-based trisureas and thioureas[26] (Fig. 30) that Gale and co-workers noticed that in some cases there would be significant efflux of chloride prior to addition of bicarbonate. This occurred particularly with the pentafluorophenyl thiourea **118** and to a lesser extent the pentafluorophenyl urea **117**. An NMR assay was developed in which ^{33}S labelled sodium sulfate was encapsulated within vesicles together with paramagnetic Mn^{2+} cations which broaden the NMR resonance of the ^{33}S and the vesicles suspended in sodium chloride solution (Fig. 31). Upon addition of a transporter capable of mediating chloride/sulfate exchange, the ^{33}S NMR resonance should appear as sulfate is transported out of the intravesicular solution containing paramagnetic Mn^{2+}. At the end of the experiment detergent was added to lyse the vesicles allowing the sulfate to again interact with the manganese ions and so the NMR resonance should be lost. The results (Fig. 31) for the tren-based compounds showed that whilst the unfluorinated compound **80** could not transport sulfate, both pentafluorophenyl derivatives **117** and **118** could. This was the first direct evidence of transmembrane sulfate transport and really a remarkable finding that such simple molecules

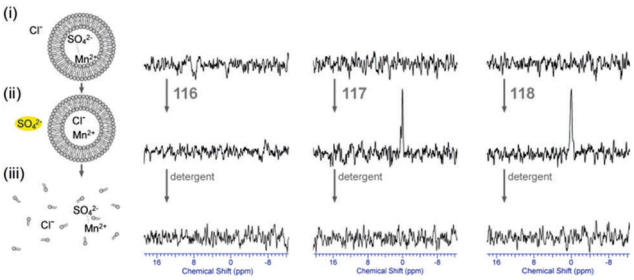

Fig. 31 ^{33}S NMR experiments indicating that receptors are able to facilitate Cl^-/SO_4^{2-} antiport (internal Mn^{2+}). All spectra were recorded in 9 : 1 water : D_2O solutions and are shown as absolute intensity. ^{33}S NMR spectra of (i) the POPC vesicles loaded with 162 mM $Na_2{}^{33}SO_4$ with $MnSO_4$ (0.5 mol% Mn^{2+} : $^{33}SO_4^{2-}$ ratio), 20 mM phosphate buffer, pH 7.2, and dispersed in 450 mM NaCl, 20 mM phosphate buffer, pH 7.2; (ii) after 2 hour incubation with transporter **116**, **117** and **118** (4 mol% transporter to lipid); (iii) after the addition of detergent to lyse all vesicles.

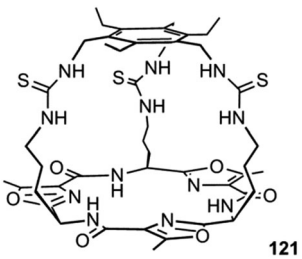

Fig. 32 The structure of compound **121**.

could facilitate the transport of this highly hydrated anion. Further studies with some more complex and preorganised sulfate receptors from Jolliffe's group *e.g.* compound **121** (Fig. 32) showed that this compound could also mediate chloride/sulfate exchange thus demonstrating the generality of this process.

Kros, Davis and co-workers have developed a method to directly visualise and quantify transport in giant unilamellar vesicles (GUVs).[34] This method employs GUVs that can be visualised using light microscopy. A version of the lucigenin assay for chloride transport is used in which sodium nitrate and lucigenin are encapsulated within the GUVs composed of 70% POPC/30% cholesterol in which a transporter such as compound **122** (Fig. 33) is pre-incorporated which are suspended is sodium nitrate solution. A pulse of sodium chloride to the extra-vesicular solution

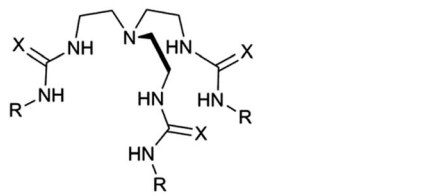

115 X=O R=C_6H_5 **116** X=S R=C_6H_5
117 X=O R=C_6F_5 **118** X=S R=C_6F_5
119 X=O R=*m*-$C_6H_3(CF_3)_2$ **120** X=S R=*m*-$C_6H_3(CF_3)_2$

Fig. 30 The structures of tripodal transporters **115–120**.

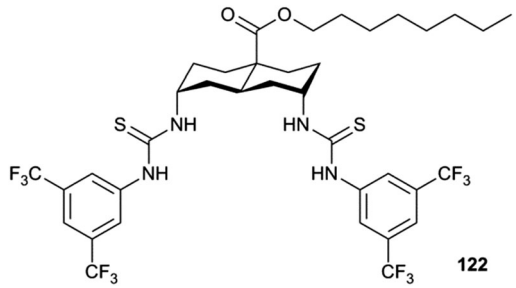

Fig. 33 The structure of decalin-based bis-thiourea **122**.

initiates transport which can be visualised using confocal fluorescence microscopy. This allowed the fluorescence of individual vesicles to be tracked and hence transport events in individual vesicles to be monitored.

Gale and co-workers have employed dynamic covalent chemistry to facilitate the transport of amino acids across lipid bilayers.[35] Squaramides had previously been shown to facilitate chloride/nitrate and chloride/bicarbonate transport across POPC lipid bilayers. Here a combination of squaramide **123** and 3,5-bistrifluoromethylbenzaldehyde were shown to facilitate the transport of glycine by both non-covalent bond formation between the squaramide and carboxylate group and reaction between the amine and the aldehyde to form either a hemiaminal or an imine. The resulting three component assembly is significantly more lipophilic than glycine and showed an enhanced rate of transport across the bilayer (Scheme 1). This was monitored using a calcein–copper complex encapsulated within the vesicle. Influx of glycine would result in sequestration of the copper from the calcein and regeneration of the calcein fluorescence. The proposed mechanism also involves the squaramide facilitating the transport of hydroxide across the lipid bilayer. It was not until the following year that the mechanism by which hydrogen bond donor anion transport dissipate pH gradients was elucidated more fully (see below).[36]

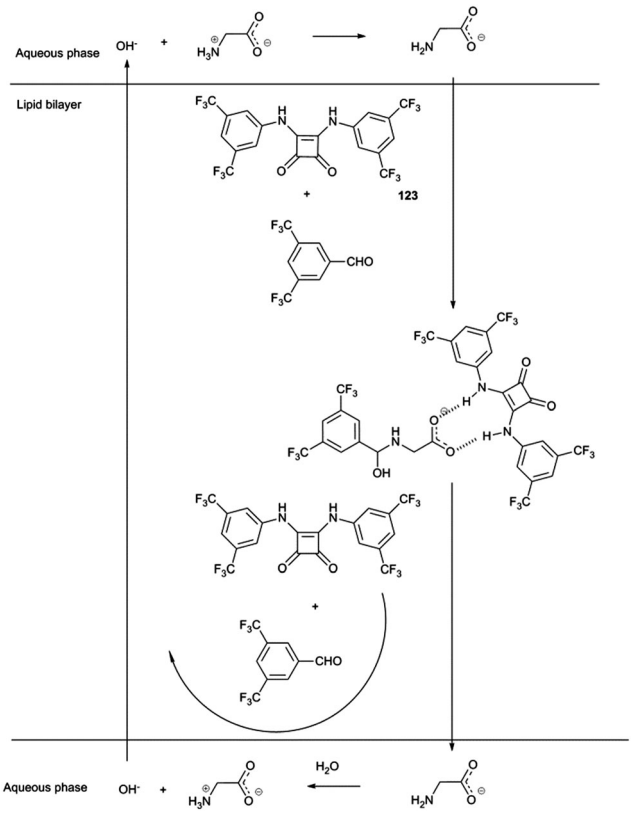

Scheme 1 Proposed mechanism for glycine transport facilitated by compound **123** and 3,5-bistrifluoromethylbenzaldehyde forming a three-component assembly involving hemiaminal formation. Alternatively imine formation is possible. OH^- transport is facilitated by compound **123** which is not shown.

Biological activity

In principle, molecules capable of facilitating transmembrane transport of anions could impact ion homeostasis of cells. This is an essential parameter involved in numerous cellular processes and thus anion selective ionophores could display a range of useful biological activities. Early studies linked the transmembrane transport activity of natural products such as prodigiosin with its cytotoxicity.[37] In this regard, Obatoclax, a synthetic prodiginine which has demonstrated its potential as ananticancer drug in the clinic, was studied by Quesada and co-workers.[38] Obatoclax **124** and related analogues (Fig. 34) were proven to be potent nitrate, bicarbonate and chloride exchangers in model liposomes. The cytotoxicity of these compounds was assayed in the small-cell lung carcinoma cell line GLC4 and was found to correlate well with their level of transmembrane transport activity. Remarkably, the BODIPY analogue **129**, inactive as anion transporter, was shown to be essentially non-toxic. This finding further support the role played by the anion transport

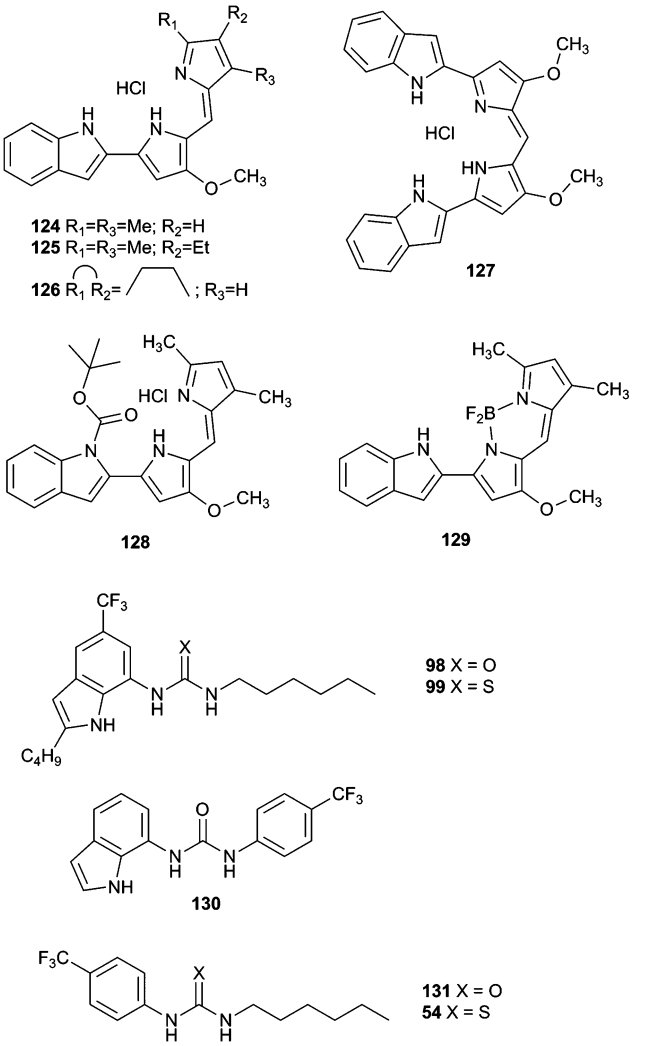

Fig. 34 Structures of obatoclax inspired transporters **124–129** and (thio)urea compounds **130** and **131**.

activity in the biological activity exerted by obatoclax and related prodiginines. This correlation between transmembrane anion transport activity and cytotoxicity was also reported by Gale and co-workers in different series of synthetic molecules. Thus, tripodal, tren-based, tris(thio)ureas **118** and **120** bearing fluorinated aryl substituents were shown to display cytotoxicity toward several cancer cell lines which correlated with their anion transport activity.[39] Similar results were observed for simpler compounds inspired by these tripodal ureas.[26] Thus, indole-based compounds were shown to induce cytotoxicity. Fluorination was proved to be a general strategy to improve the activity and cytotoxicity of small molecule anion transport agents. IC_{50} values of 6–23 μM on GLC4, A375 cancerous cell lines were found for these derivatives. These values were significantly lower than the cytotoxicity exerted in the non-cancerous cell line MCF10A.

The activity of calix[4]pyrrole-strapped diamides **132** and **133** was studied in a panel of cell lines by Gale, Sessler and Shin.[40] These compounds were shown to mediate both chloride and sodium influx as well as to induce apoptosis *via* a caspase-dependent pathway. The caspase activation is related to an enhancement of cellular ROS levels, and the release of cytochrome *c* from the mitochondria (Fig. 35).

Tambjamine alkaloids represent models to explore the relationships between facilitated anion transport and the cytotoxicity exerted by these compounds because their synthetic accessibility.[21] Following the study of the cytotoxicity of these compounds, a detailed study of the anti-cancer effect of tambjamine analogues **134** and **135** was carried out in several lung cancer cell lines by Pérez-Tomás and co-workers.[41] Treatment of A549 cells with these derivatives led to cytoplasmic vacuolization as a result of loss of mitochondrial potential and mitochondrial swelling. This could also trigger mitophagy (mitochondrial autophagy). Indeed, accumulation of LC3II protein indicated that autophagy was being triggered by the treatment with these tambjamine analogues. On the other hand, lysosome alkalinization results in autophagy blockage and accumulation of autophagosomes and autolysosomes. All these processes led to cellular stress, resulting in activation of p38 Mitogen-Activated Protein Kinase (MAPK) in A549 cells in a dose–response manner. This signal has been reported to activate apoptosis and small activation of apoptotic markers was observed. The fact that cell viability was not recovered when a pan-caspase inhibitor (10 l M Z-VAD-FMK) was added before treatment with these derivatives suggested that although apoptosis is being triggered by these tambjamine analogues, this process is not entirely responsible for the cytotoxic effect induced by these compounds, and necrosis plays an important role as cell death mechanism. The related synthetic tambjamine analogues **137–139** were tested against lung cancer stem cells (CSC).[42] This cancer cell population is noted because of its resistance to chemotherapy and its involvement in tumour recurrence and metastasis. CSC are characterised by a depolarised membrane and facilitated anion transport could impact the membrane polarisation state. Using a fluorescence assay based on a FRET of genetically encoded transmembrane proteins, it was demonstrated that compounds **137** and **138** hyperpolarised the membrane. Remarkably this effect was not observed for compound **139**. Thus compound **139** resulted an appropriate negative control, being structurally very similar yet inactive as a transporter. Compounds **137** and **138** proved highly active against lung cancer CSC, inducing differentiation and elimination of CSC (Fig. 36).

Disruption of autophagy was also reported for synthetic anion transporters containing squaramide moieties. In a detailed study, Shin, Gale, Sessler and colleagues demonstrated that squaramide-based transporter **18** raised lysosomal pH.[43] This pH is not suitable for lysosome enzymatic function, leading to autophagy impairment. In addition, an increase of chloride and sodium cytosolic concentrations facilitated by **18** lead to cytochrome *c* release from the mitochondria into the cytosol, promoting caspase-dependent apoptosis.

Another important area of research focus in the use of these compounds as protein mimics. For instance, in the case of

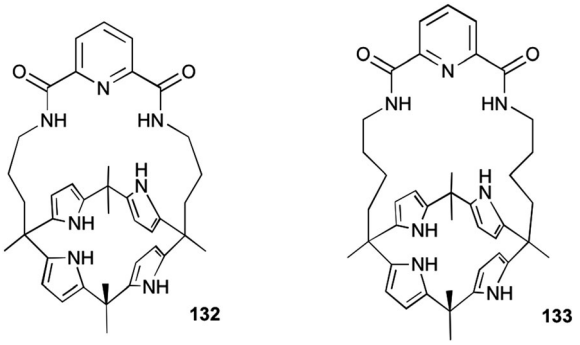

Fig. 35 Diamide straped calixpyrrole **132** and **133**.

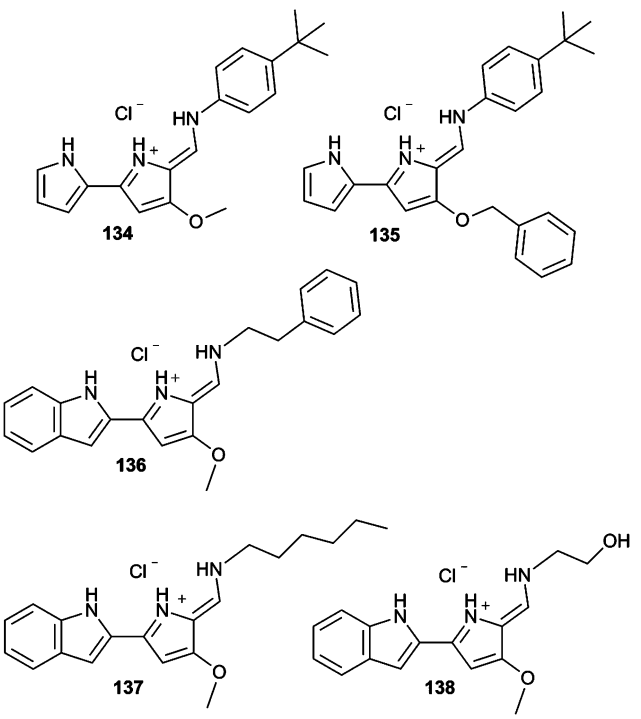

Fig. 36 Tambjamine inspired receptors **134–138**.

dysfunction of natural transmembrane transport mechanisms, anion selective transporters could restore the missing activity representing a valuable therapeutic approach for related conditions, notably cystic fibrosis (CF). However, perturbation of pH gradients within cells has been linked to apoptosis – an undesirable outcome when using a compound to replace the function of a faulty ion channel.

The mechanism by which neutral hydrogen bond donating anion transporters can dissipate pH gradients across lipid bilayer membranes has been elucidated by Gale and co-workers.[36] They found that depending on the acidity of the transporter, more acidic compounds could function as weak acid protonophores, more weakly acidic compounds may transport hydroxide or alternatively transport fatty acid carboxylate groups through the membrane to the other side where they can be protonated and then diffuse back across the lipid bilayer as the carboxylic acid.[44] Gale also developed assays to measure the Cl^- *vs.* H^+ selectivity of transporters finding that encapsulating binding sites (such as that found in compound **139** conferred a degree of selectivity for chloride transport) but that most hydrogen bond donor anion transporters tested are unselective. Compound **139** was tested in human cancer cells and in epithelial cells. It was found not to perturb lysosomal pH gradients in the former but to transport chloride through the cell membranes in the latter. Further studies with encapsulated binding sites within calix[4]pyrrole macrocycles **4–6** showed that these compounds also facilitate selective chloride transport with a degree of selectivity remaining even in the presence of significant quantities of fatty acids.[35] Gale and co-workers also measured the Cl^- *vs.* F^- selectivity of these compounds using a fluoride selective electrode to monitor fluoride transport. This group found that calix[4]pyrroles **4** and **5** with the shorter straps were selective for fluoride over chloride transport (Fig. 37).[45]

Another area of interest is the biocide activity of anion selective transmembrane transporters. Indeed, a number of natural ionophores (which are cation selective) found applications as antibiotics and anticoccidiostates.[46] Membrane permeabilization to anions should have similar effects on these organisms yet this is an understudied area of research.

Smitzer and co-workers reported the benzimidazolium salt **140** (Fig. 38), which was identified as a chloride transporter using the lucigenin fluorescence assay with an EC_{50} of 0.46 mol%.[47] The antibacterial activity of this benzimidazolium salt was thus evaluated in the presence of Gram-negative *E. coli* and

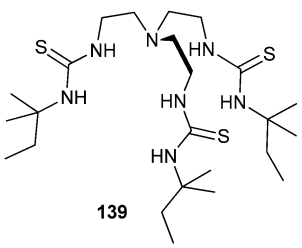

139

Fig. 37 Chloride selective transporter **139** possesses an encapsulating binding site.

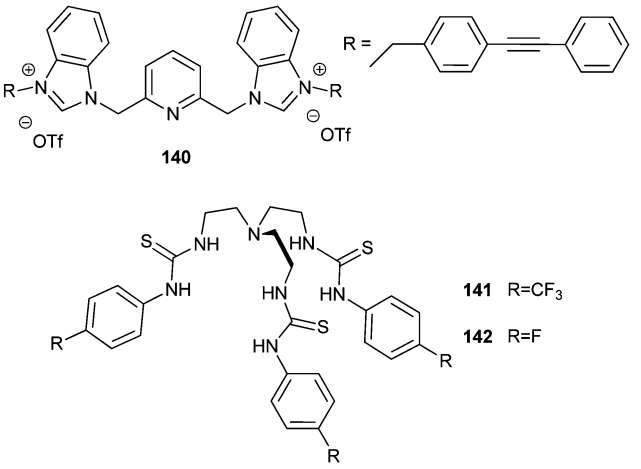

140

141 R=CF_3

142 R=F

Fig. 38 Anion selective transporters tested as antimicrobial agents.

Gram-positive *B. thuringiensis* strain. MICs of 25 μM for *E. coli* DH5-α, 10 μM for *E. coli* SK037 and 2 μM for *B. thuringiensis* were found. The antimicrobial activity of related, less potent chloride carriers was found to be considerably lower. Compound **140** was found to disrupt the integrity and the potential of the bacterial membranes, and this is likely the origin of its antibacterial activity. Remarkably, the low toxicity against eukaryotic cells as well as low haemolytic activity bodes well for the future development of this class of compounds as antimicrobial agents.

The inhibition of the growth of *S. aureus in vitro* by anion transporters was demonstrated by Francesconi, Gale, Roelens, Sessler and co-workers. Importantly, this activity was also demonstrated against methicillin-resistant Staphylococcus aureus (MRSA) strains, Mu50 and HP117. Thus, potent tris-thiourea tren-based transporters bearing fluorinated substituent such as **118**, **141** and **142** (Fig. 38), were found to have MIC in the low micromolar range (0.93–1.78 mg mL^{-1} for the Mu50 *S. aureus*).[48]

Yang and co-workers have focused their studies on isophthalamide-like small molecules. Compound **143** was found to mediate chloride transport in both liposomes and live cells.[49] Using whole cell patch clamp recordings in HEK293 cells **143** was found to form anion selective channels with an anion transport activity following the order $NO_3^- > I^- > Br^- > Cl^- > F^-$. To investigate the ability of compound **143** to restore chloride permeability in cells, whole cell currents were measured in the presence of this compound for cells derived from normal human bronchial epithelia and bronchial epithelia of CF patients. These experiments revealed that this compound increase the chloride permeability of CF airway epithelial cells. This increase was found to be larger than that induced by forskolin in normal human epithelial cells, suggesting an alternative mechanism for chloride transport.

The isophthalamide-like molecules were found to mediate chloride and bicarbonate transport in liposomes.[50] Patch clamp experiments indicated the formation of functional chloride channels by **144**. The ability of this compound to augment chloride permeability in Calu-3 and CFBE41o (with homozygous F508 mutation)

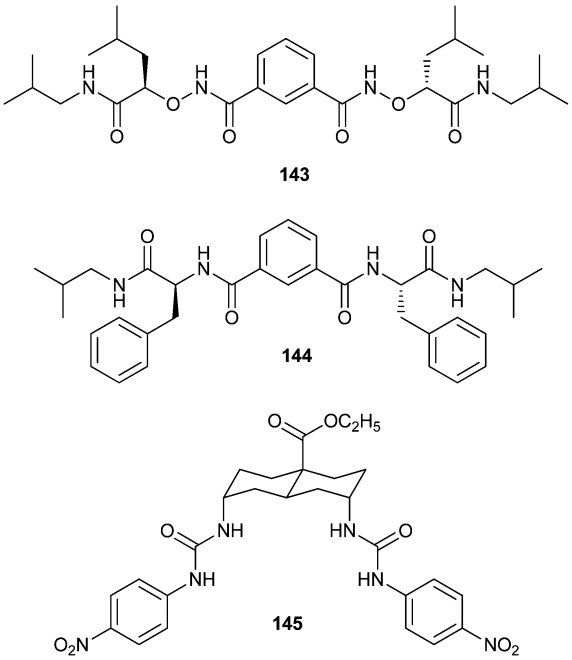

Fig. 39 Anion transporters capable of inducing chloride transport in living cells.

epithelial monolayers was tested with the Ussing chamber based short-circuit method. In both cases this compound was found to induce chloride dependent short circuit current increases.

Anion transport in living cells can also be monitored by fluorescence methods. For instance, FRT cells stably expressing the halide sensor YFP-H148Q/I152L (YFP-FRT cells) can be used to monitor halide transport without using specialist electrophysiological apparatus.[51] Using this fluorescence based method Davis, Sheppard and co-workers screened a wide range of synthetic anion transporters.[52] From these studies, the bisureiodododecalin **145** was identified as a promising candidate, facilitating iodide transport efficiently. Moreover, this compound is able to incorporate to cell membranes readily and at effective dosages did not showed significant toxicity. Further electrophysiological studies confirmed these results. Chloride currents in YFP-FRT epithelia were measured using the Ussing chamber technique. A robust increase in I^{Cl} apical was observed. For comparison purposes, chloride current intensities in MDCK epithelia were also measured after forskolin stimulation. The maximum current induced was found to be roughly half that of natural CFTR measured for the MDCK epithelia (Fig. 39).

Non-classical transporters

Most synthetic anion transporters rely on standard hydrogen bond donors such as amide or urea NH groups as to bind anions for their subsequent transport across the bilayer membrane. Below, we describe some of the most important papers that have appeared since 2010 that use non-classical interactions to achieve transmembrane transport of anions.

Over the past decade, CH hydrogen bonds have become increasingly recognized to be an important structural motif in supramolecular chemistry, nanochemistry and molecular biology. Thus, some CH donors, such as those that occur in the triazole group, form relatively strong CH hydrogen bonds. In recent years, the use of CH hydrogen bonds as a design element for the development of selective anion transporters has taken hold. Below, we describe two such leading studies wherein CH hydrogen bonds were used to develop transmembrane anion transporters. The first example of a CH hydrogen-bonding transporter was reported in 2014 by Jiang, Hou and colleagues.[53] They described a pre-organized aryltriazole foldamer **146** that can bind anions using an array of C–H hydrogen bond donors (Fig. 40). Four intramolecular NH···N hydrogen bonds between amides and triazoles on its periphery fix **146** into a conformation that points five C–H bonds into a crescent-shaped cleft. The authors reasoned that such a pre-organized structure should favor the anion binding needed for transmembrane transport. The proposed conformation of **146** was confirmed by X-ray crystallography and also in solution using NOEs. The authors prepared a key control, as compound **147** lacks two of the intramolecular hydrogen-bonds that rigidify **146**. Indeed, **147** is conformationally flexible as NOEs indicated free rotation about the single bonds between triazoles and neighboring aromatic rings. NMR titrations in CD_2Cl_2 showed that fully pre-organized receptor **146** had a 1 : 1 binding constant for $TBA^+ Cl^-$ ($757\ M^{-1}$) that was 8-fold stronger than that for the partly pre-organized receptor **147** ($91\ M^{-1}$). These binding studies showed that use of all possible C–H···anion interactions in the binding pocket relies on pre-organization of foldamer **146** by hydrogen-bond array on the receptor's periphery. The transmembrane Cl^- transport activity of the two compounds was measured with EYPC LUVs using the classic lucigenin fluorescence assay, in the presence of catalytic amounts of the K^+-carrier valinomycin. Valinomycin enables a K^+ uniport process that helps the anionophore (**146** or **147**) facilitate Cl^- uniport in an overall K^+/Cl^- symport process. Foldamer **146** was a better Cl^- transporter than control **147**. Thus, addition of **146** (0.75% relative to EYPC) and valinomycin (0.002%) to a LUV suspension led to a 97% increase in lucigenin fluorescence in the 12 min experiment, whereas the same amount of compound **147** increased the fluorescence by

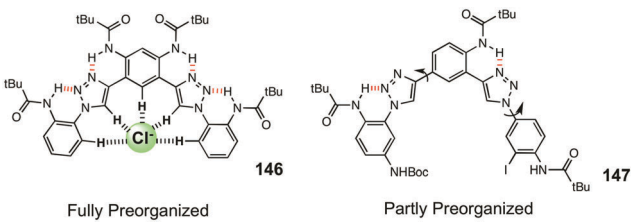

Fig. 40 The aryltriazole foldamer **146** is fully pre-organized by four contiguous hydrogen bonds on its periphery. Receptor **146** favours a conformation that is optimal for anion binding, and subsequent transmembrane anion transport, by the use of CH···anion hydrogen-bonds. The control compound **147**, because it lacks the same degree of pre-organization as **146**, is conformationally more flexible and does not bind or transport chloride anion as well as foldamer **146**.

just 39% over the same time. Other transport experiments revealed that foldamer **146** functioned as a mobile carrier, had a respectable EC_{50} value of 0.09% relative to EYPC lipid and had a Hill coefficient (n = 1.3) indicative of a unimolecular Cl^- transporter. This study demonstrated that conformational control of aryltriazole foldamers such as **146** can be used to bind and transport Cl^- using CH···anion hydrogen-bonds. The authors concluded with the suggestion that switching elements might be incorporated so as to modulate foldamer conformation, and enable the reversible uptake and release of anions.

Recently the Pittelkow and A. P. Davis groups reported together on the anion transport properties of lipophilic biotin[6]urils, macrocyclic receptors that use only CH hydrogen bonds to bind anions within their central cavity (Fig. 41).[54] Both ^{1}H NMR and ITC titrations revealed that the biotin methyl ester **148** has a ~100-fold selectivity for binding Cl^- *vs.* HCO_3^- in CD_3CN. The authors noted that HCO_3^- and NO_3^-, anions with similar shapes but different basicities, had similar affinities for receptor **148**. They attributed this result to the unique character of the CH···anion hydrogen-bond, which has much less of an electrostatic component than conventional hydrogen-bonds. Butyl ester **149** was a particularly effective transmembrane anion transporter, as judged by the classical "lucigenin assay" in POPC:cholesterol liposomes. Lipophilicity was an important feature, since the butyl ester **149** was a better transporter than the ethyl or methyl esters. Butyl ester **149** was a relatively potent Cl^- transporter, as it showed a $t_{1/2}$ = 180 s at the low carrier/lipid loading of 1 : 2500. Notably, **149** was highly selective for transporting Cl^- *vs.* HCO_3^- in this liposome model. Thus, while **149** catalyzed efficient Cl^-/NO_3^- transmembrane it hardly promoted any observable Cl^-/HCO_3^- exchange over background. The authors noted that this high degree of Cl^-/HCO_3^- selectivity for biotin[6]uril **149**, which uses only CH hydrogen-bonds to coordinate the target anion, was in marked contrast with receptors that use conventional hydrogen-bond donors such as urea and amide NH groups. They attributed this selectivity to the relatively "soft" nature of CH as a hydrogen bond donor, which would favour binding of more hydrophobic anions, such as Cl^- and NO_3^-, over the more basic HCO_3^-. The Cl^-/HCO_3^- selectivity shown by biotin[6]uril ester **149** is potentially important for biological applications that require specific Cl^- transport *vs.* HCO_3^- transport.

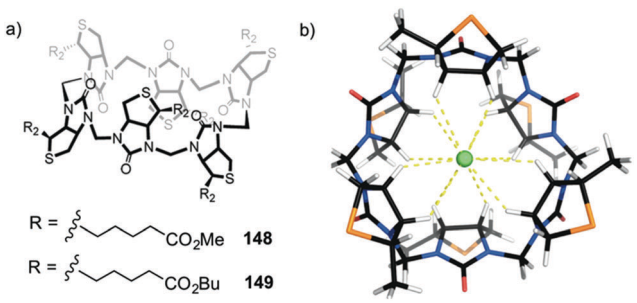

Fig. 41 Macrocyclic biotin[6]uril esters use CH···anion hydrogen-bonds to selectively transport Cl^- across lipid membranes. (a) Structures of biotin[6]uril esters **148** and **149**. The lipophilic butyl ester **149** is a better anion transporter than methyl ester **148**. (b) An energy-minimized model of the biotin[6]uril macrocycle's core showing the CH···Cl^- hydrogen-bonds. Reproduced from ref. 54 which is published under a CC-BY license.

The anion–π interaction, an attractive force between an anion and an electron-deficient aromatic π system, is a noncovalent bond finding increasing use in the construction of functional supramolecular systems. To bind anions with aromatic surfaces a compound's quadrupole moment has to be positive instead of negative. This reversal in quadrupole moment is accomplished by substituting the aromatic ring with strong electron-withdrawing groups. In earlier work, Matile and colleagues had shown that oligomers of π-acidic naphthalenediimide (NDI), dubbed "anion–π slides", catalyzed anion transport across lipid bilayers, presumably by enabling anions to hop from one π-acidic site to the next as they move across the bilayer.[55] Although these early studies on the rigid-rods suggested that anion–π interactions were responsible for transport, these authors sought more convincing evidence for the functional relevance of these non-classical interactions.

To address the fundamental question of whether anion–π interactions are responsible for transmembrane anion transport, Matile and colleagues "deconstructed" the NDI rods to give a family of simpler NDI models **150–152**.[56] This work has become a landmark in the field, as both experiment and computation demonstrated that non-classical interactions can be used to effect transmembrane anion transport. First, the authors used mass spectrometry to measure relative affinities of anions binding to **150–152**; competition experiments revealed a Cl^- binding selectivity of **152** ≫ **151** > **150**. These results showed that increasing the NDI's π acidity, along with minimizing steric congestion near the anion binding site, provided a receptor **152** with optimal anion binding affinity. The Cl^- anion transport activity of NDI monomers **150–152** was tested in EYPC liposomes using the standard HPTS fluorescence assay and compound **152** was found to be the most active of the compounds, showing significant Cl^- transport activity even at nM concentrations (EC_{50} = 330 nM). Computational models of NDI **152**, an analogue with 2 electron-withdrawing cyano groups, showed Cl^- binding to the π-acidic surface and stabilized by C–H···anion hydrogen-bonds with a peripheral phenyl group. The major accomplishment in this study was to correlate the strength of the non-covalent anion–π interaction for a particular compound with its efficiency as a transmembrane anion transporter. Thus, the higher a compound's affinity for binding anions then the better was its anion transport activity, supporting the hypothesis that it is indeed the anion–π interactions that account for the anion-transport function displayed by the rigid rods in Matile's earlier papers, and by the π-acidic monomers **150–152** described in this present study (Fig. 42).

Halogen bonding, the non-covalent interaction between an electron-deficient halogen and a neutral or anionic Lewis base, is being increasingly used in supramolecular chemistry, catalysis and, now, in anion transport. Matile and colleagues prepared a series of ditopic calix[4]arene receptors, including **153–155**, with different halogen substitution patterns on the calixarene's lower rim. These ion-pair receptors selectively bind tetramethylammonium

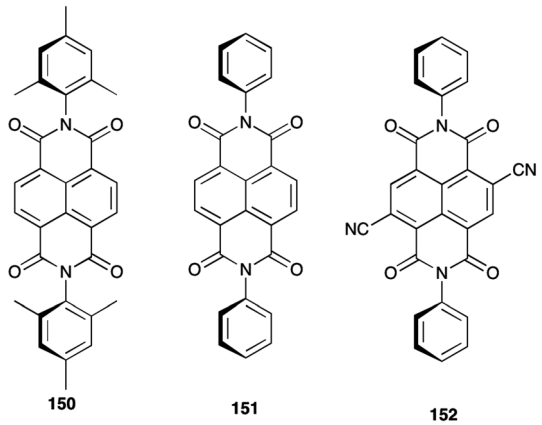

	150	151	152
Cl^- Binding (ESI-MS)	+	++	+++
Cl^- Transport (EC_{50} μM)	150	27	0.33

Fig. 42 Summary of anion binding and transport data for NDIs **150–152**.

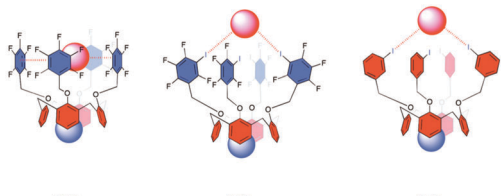

	153	154	155
Cl^- Transport (EC_{50} μM)	25	1000	32
E_{int} (Kcal/mol)	-58.3	-70.9	-59.7

Fig. 43 Summary of anion transport data and DFT calculated energies to Cl-anion for calixarenes **153–155**.

(TMA^+) cations within the calixarene's upper rim, while the lower rim coordinates chloride anion. This study's major goal was to use these calix[4]arenes to systematically evaluate the contributions of various non-classical interactions, including CH···anion hydrogen bonds, anion–π interactions and anion–halogen bonds to the transmembrane transport of anions.[57] Using their standard HPTS assays, which monitors intravesicular pH, the authors demonstrated that calixarenes **153–155** catalyze transmembrane Cl^-/OH^- exchange with varying efficiencies. Calixarene **153**, with its pentafluoroaryl groups, proved to be the best Cl^- transporter in the series, with a relatively low EC_{50} value of 25 μM. DFT models of the **153**·TMACl complex indicated a binding energy of −58.3 kcal mol^{-1} and revealed a structure wherein 3 of the 4 pentafluoroaryl groups in **153** formed anion–π interactions with bound Cl^-. Significantly, a single-atom F to I mutation of **153** to give the *m*-iodo analogue **154** resulted in near complete loss of Cl^- transport activity (EC_{50} for **154** = 1000 μM). The authors concluded that this drop-off in anion transport ability was because this *m*-iodo analogue **154** uses a combination of anion–π and anion–halogen interactions to actually bind Cl^- too strongly to allow effective anion transport. In support of this hypothesis, ^{19}F NMR titrations showed that receptor **154** (but not active transporters **153** or **155**) binds TBACl in acetone-d_6. Moreover, DFT calculations indicated a greater binding energy of −70.9 kcal mol^{-1} for the **154**·TMACl complex as compared to that for the **153**·TMACl. The authors reasoned that weakening Cl^- binding by removing the anion–π interactions, while keeping the anion–halogen bonds, should restore transmembrane Cl^- transport by analogue **155**. Indeed, replacing all the –F atoms in **154** with –H atoms, gave an analogue **155** with an EC_{50} value of 32 μM, more than 30 times lower than that of **154**. Presumably, it is the anion–halogen bonds in **155** that enable functional transport across lipid bilayers (Fig. 43).

In another nice demonstration of the importance of anion–π interactions, Ballester, Matile and colleagues reported that calix[4]pyrrole derivatives **156–158**, containing aryl substituents at two opposing *meso*-positions promoted selective transmembrane transport of nitrate over other anions (Fig. 44).[58] Using NMR titration data they determined the strength of the nitrate–π interaction as a function of the *meso*-substituent and found that the calix[4]pyrroles' affinity for nitrate correlated well with the electrostatic surface potential for a particular aryl group. The 3,5-dinitrophenyl analogue **158**, the most π-acidic compound in the series, had the highest binding constant for nitrate. An X-ray structure of the complex $TBA^+[\mathbf{158}\cdot NO_3]^-$ showed the nitrate anion bound between the two opposing *meso*-aryl walls and oriented perpendicular to the rings. The ability of calix[4]pyrrole derivatives to transport anions across EYPC LUVs was evaluated using the standard HPTS assay. All calix[4]pyrroles tested showed Cl^- transport ability, but those analogues with the most π-acidic surfaces, namely **157** and **158**, were the best Cl^- transporters. Importantly, they also showed transport selectivity for the trigonal planar NO_3^- anion *vs.* Cl^-. This remarkable nitrate transport selectivity by **157** and **158** was attributed to (1) the specific nitrate–π interactions implied by the X-ray crystal structure and (2) the ability of the π-acidic walls to effectively sequester nitrate as it is moved across the hydrophobic lipid bilayer by the calix[4]pyrrole carrier.

It is not just structurally complex carriers, such as calixarenes and calixpyrroles, that can use non-classical interactions as a driving force for anion transport. In an interesting study, Matile and colleagues showed that low-molecular weight compounds, such as **159** (and even a 1-carbon carrier **160**) with halogen bond acceptors could function as transmembrane anion transporters.[59]

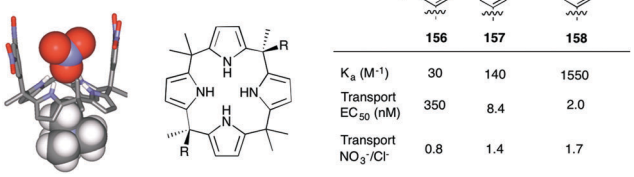

	156	157	158
K_a (M^{-1})	30	140	1550
Transport EC_{50} (nM)	350	8.4	2.0
Transport NO_3^-/Cl^-	0.8	1.4	1.7

Fig. 44 Left: X-ray crystal structure of **158**·NO_3^- complex. Right: Summary of anion binding and transport data for calix[4]pyrroles **156–158**.

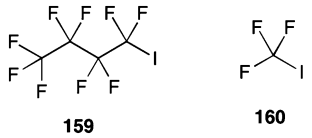

159 160

Fig. 45 Minimalistic halogen-bonding anion transporters **159** and **160**.

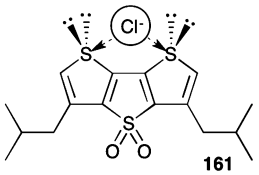

161

Fig. 46 Chalcogen bonding transporter **161**.

DFT calculations revealed that an individual Cl^- could be encased in a hydrophobic cocoon by six molecules of the perfluoroiodide **160**, thus facilitating the membrane transport process by protecting the charged anion from the non-polar lipid environment. HPTS fluorescence assays revealed a remarkably low value of EC_{50} = 21.6 μM for **160**, with a Hill coefficient of n = 4.7, which is consistent with the DFT calculations for formation of halogen bonded capsules. Although trifluoroiodomethane **160** is a relatively poor anion transporter, it is remarkable that it works at all since it contains just a single carbon. Finally, one attractive feature of anion carriers such as **160** is their innate hydrophobicity and complete lack of hydrophilic hydrogen bonding groups, which can cause aggregation or encounter dehydration penalties when entering a lipophilic environment (Fig. 45).

Much like halogen bonds, chalcogen bonds form upon electron donation from a Lewis base into the Lewis acidic σ hole found in electron-deficient sulfur atoms. Very recently, Matile and colleagues introduced synthetic anion transporters that use chalcogen bonds to coordinate anions.[60] Electron-deficient dithieno[3,2-*b*;2′,3′-*d*]thiophenes (DTTs) were shown to chelate anions using the Lewis acidic σ holes on two adjacent sulfur atoms that were located in a constrained binding site. Both the strength of anion binding in solution and the rates of anion transport across lipid bilayers increased with the increasing electron deficiency of the sulfur acceptor atoms in a series of DTT anionophores. The best Cl^- anion transporter was compound **161** (EC_{50} = 1.9 μM), whose σ holes on the sulfur atoms were enhanced by substitution of the thiophene rings with electron-withdrawing cyano groups and a sulfoxide unit. The authors noted that DTT ligands such as **161**, which use non-classical chalcogen bonds to coordinate and transport anions, complement the 2,2′-bipyrrole unit, a truly classic hydrogen bonding motif for anion binding and transport (Fig. 46).

Conclusions

In the last few years there has been a rapid progress in the development of anion selective transmembrane transporters. Highly efficient systems both inspired in naturally occurring derivatives and *de novo* designed systems have appeared. Important insights into transport mechanism and transporter selectivity have been obtained. Importantly, supramolecular transmembrane anion transport is making the leap from model systems to cells. Early studies show great promise. A range of anion transporters that can dissipate pH gradients have been prepared and shown reduce the viability of human cancer cell lines. Recent experiments show that one mechanism that may be responsible for this is disruption of autophagy. Meanwhile compounds that are selective chloride transporters are beginning to be developed and shown to transport chloride through epithelial cell membranes. Compounds that transport chloride but do not perturb pH gradients within cells may be candidates to replace the function of faulty anion channels in diseases like cystic fibrosis. The chasm between studies in model membranes and applications of anion transporters in biological systems has been bridged and a new application in supramolecular medicinal chemistry is in sight.

Acknowledgements

PAG thanks the University of Sydney and the Australian Research Council (DP170100118) for funding. JTD thanks the Office of Basic Energy Sciences, U.S. Department of Energy (DE-FG02-98ER14888) for funding. RQ thanks Consejería de Educación de la Junta de Castilla y León (BU340U13 and BU092U16) and La Marató de TV3 Foundation (20132730) for funding.

References

1 (*a*) D. C. Gadsby, *Nat. Rev. Mol. Cell Biol.*, 2009, **10**, 344–352; (*b*) B. Hille, *Ion Channels of Excitable Membranes*, Sinauer Associates, Sunderland, MA, 3rd edn, 2001.
2 (*a*) F. M. Ashcroft, *Nature*, 2006, **440**, 440–447; (*b*) E. Marban, *Nature*, 2002, **415**, 213–218; (*c*) M. J. Ackerman and D. E. Clapham, *N. Engl. J. Med.*, 1997, **336**, 1575–1586.
3 (*a*) F. Ratjen, S. C. Bell, S. M. Rowe, C. H. Goss, A. L. Quittner and A. Bush, *Nat. Rev. Dis. Primers*, 2015, **1**, 15010; (*b*) D. C. Gadsby, P. Vergani and L. Csanady, *Nature*, 2006, **440**, 477–483; (*c*) M. J. Welsh and A. E. Smith, *Cell*, 1993, **73**, 1251–1254; (*d*) J. R. Riordan, J. M. Rommens, B. S. Kerem, N. Alon, R. Rozmahel, Z. Grzelczak, J. Zielenski, S. Lok, N. Plavsic, J. L. Chou, M. L. Drumm, M. C. Iannuzzi, F. S. Collins and L. C. Tsui, *Science*, 1989, **245**, 1066–1073; (*e*) P. M. Quinton, *Nature*, 1983, **301**, 421–422.
4 F. M. Ashcroft, *Ion Channels and Disease*, Academic Press, 2000.
5 D. K. Smith, *J. Chem. Educ.*, 2005, **82**, 393–400. For recent developments in anion receptor chemistry including transmembrane anion transport in cells see: P. A. Gale, E. N. W. Howe and X. Wu, *Chem*, 2016, **1**, 351–422.
6 P. A. Gale, C. C. Tong, C. J. Haynes, O. Adeosun, D. E. Gross, E. Karnas, E. M. Sedenberg, R. Quesada and J. L. Sessler, *J. Am. Chem. Soc.*, 2010, **132**, 3240–3241.
7 M. Yano, C. C. Tong, M. E. Light, F. P. Schmidtchen and P. A. Gale, *Org. Biomol. Chem.*, 2010, **8**, 4356–4363.

8 I. W. Park, J. Yoo, B. Kim, S. Adhikari, S. Kuk Kim, Y. Yeon, C. J. E. Haynes, J. L. Sutton, C. C. Tong, V. M. Lynch, J. L. Sessler, P. A. Gale and C. Lee, *Chem. – Eur. J.*, 2012, **18**, 2514–2523.
9 C. J. E. Haynes, S. J. Moore, J. R. Hiscock, I. Marques, P. J. Costa, V. Félix and P. A. Gale, *Chem. Sci.*, 2012, **3**, 1436–1444.
10 N. Busschaert, I. L. Kirby, S. Young, S. J. Coles, P. N. Horton, M. E. Light and P. A. Gale, *Angew. Chem., Int. Ed.*, 2012, **51**, 4426–4430.
11 R. B. P. Elmes, N. Busschaert, D. D. Czech, P. A. Gale and K. A. Jolliffe, *Chem. Commun.*, 2015, **51**, 10107–10110.
12 E. N. W. Howe, N. Busschaert, X. Wu, S. N. Berry, J. Ho, M. E. Light, D. D. Czech, H. A. Klein, J. A. Kitchen and P. A. Gale, *J. Am. Chem. Soc.*, 2016, **138**, 8301–8308.
13 S. J. Edwards, H. Valkenier, N. Busschaert, P. A. Gale and A. P. Davis, *Angew. Chem.*, 2015, **127**, 4675–4679.
14 B. A. McNally, A. V. Koulov, B. D. Smith, J. B. Joos and A. P. Davis, *Chem. Commun.*, 2005, 1087–1089.
15 C. R. Yamnitz, S. Negin, I. A. Carasel, R. K. Winter and G. W. Gokel, *Chem. Commun.*, 2010, **46**, 2838–2840.
16 X. Wei, G. Zhang, Y. Shen, Y. Zhong, R. Liu, N. Yang, F. Y. Almkhaizim, M. A. Kline, L. He, M. Li, Z.-L. Lu, Z. Shao and B. Gong, *J. Am. Chem. Soc.*, 2016, **138**, 2749–2754.
17 T. Saha, S. Dasari, D. Tewari, A. Prathap, K. M. Sureshan, A. K. Bera, A. Mukerjee and P. Talukdar, *J. Am. Chem. Soc.*, 2014, **136**, 14128–14135.
18 T. Saha, A. Gautam, A. Mukerjee, M. Lahiri and P. Talukdar, *J. Am. Chem. Soc.*, 2016, **138**, 16443–16451.
19 A. Vargas Jentzsch and S. Matile, *J. Am. Chem. Soc.*, 2013, **135**, 5302–5303.
20 L. Chen, W. Si, G. Tang, Z.-T. Li and J.-L. Hou, *J. Am. Chem. Soc.*, 2013, **135**, 2152–2153.
21 V. Saggiomo, S. Otto, I. Marques, V. Félix, T. Torroba and R. Quesada, *Chem. Commun.*, 2012, **48**, 5274–5276.
22 N. Busschaert, S. J. Bradberry, M. Wenzel, C. J. E. Haynes, J. R. Hiscock, I. L. Kirby, L. E. Karagiannidis, S. J. Moore, N. J. Wells, J. Herniman, G. J. Langley, P. N. Horton, M. E. Light, I. Marques, P. J. Costa, V. Félix, J. G. Frey and P. A. Gale, *Chem. Sci.*, 2013, **4**, 3036–3045.
23 M. J. Spooner and P. A. Gale, *Chem. Commun.*, 2015, **51**, 4883–4886.
24 N. Busschaert, P. A. Gale, C. J. E. Haynes, M. E. Light, S. J. Moore, C. C. Tong, J. T. Davis and W. A. Harrell Jr., *Chem. Commun.*, 2010, **46**, 6252–6254.
25 N. J. Andrews, C. J. E. Haynes, M. E. Light, S. J. Moore, C. C. Tong, J. T. Davis, W. A. Harrell Jr. and P. A. Gale, *Chem. Sci.*, 2011, **2**, 256–260.
26 N. Busschaert, M. Wenzel, M. E. Light, P. Iglesias-Hernández, R. Pérez-Tomás and P. A. Gale, *J. Am. Chem. Soc.*, 2011, **133**, 14136–14148.
27 H. Valkenier, C. J. E. Haynes, J. Herniman, P. A. Gale and A. P. Davis, *Chem. Sci.*, 2014, **5**, 1128–1134.
28 C. J. E. Haynes, N. Busschaert, I. L. Kirby, J. Herniman, M. E. Light, N. J. Wells, I. Marques, V. Félix and P. A. Gale, *Org. Biomol. Chem.*, 2014, **12**, 62–72.
29 S. Hussain, P. R. Brotherhood, L. W. Judd and A. P. Davis, *J. Am. Chem. Soc.*, 2011, **133**, 1614–1617.
30 J. A. Cooper, S. T. G. Street and A. P. Davis, *Angew. Chem., Int. Ed.*, 2014, **53**, 5609–5613.
31 S. J. Moore, M. Wenzel, M. E. Light, R. Morley, S. J. Bradberry, P. Gómez-Iglesias, V. Soto-Cerrato, R. Pérez-Tomás and P. A. Gale, *Chem. Sci.*, 2012, **3**, 2501–2509.
32 S. Bahmanjah, N. Zhang and J. T. Davis, *Chem. Commun.*, 2012, **48**, 4432–4434.
33 N. Busschaert, L. E. Karagiannidis, M. Wenzel, C. J. E. Haynes, N. J. Wells, P. G. Young, D. Makuc, J. Plavec, K. A. Jolliffe and P. A. Gale, *Chem. Sci.*, 2014, **5**, 1118–1127.
34 H. Valkenier, N. López Mora, A. Kros and A. P. Davis, *Angew. Chem., Int. Ed.*, 2015, **54**, 2137–2141.
35 X. Wu, N. Busschaert, N. J. Wells, Y.-B. Jiang and P. A. Gale, *J. Am. Chem. Soc.*, 2015, **137**, 1476–1484.
36 X. Wu, L. W. Judd, E. N. W. Howe, A. M. Withecombe, V. Soto-Cerrato, H. Li, N. Busschaert, H. Valkenier, R. Perez-Tomas, D. N. Sheppard, Y.-B. Jiang, A. P. Davis and P. A. Gale, *Chem*, 2016, **1**, 127–146.
37 J. L. Sessler, L. R. Eller, W.-S. Cho, S. Nicolaou, A. Aguilar, J. T. Lee, V. M. Lynch and D. J. Magda, *Angew. Chem., Int. Ed.*, 2005, **44**, 5989–5992.
38 B. D. de Greñu, P. I. Hernandez, M. Espona, D. Quiñonero, M. E. Light, T. Torroba, R. Pérez-Tomás and R. Quesada, *Chem. – Eur. J.*, 2011, **17**, 14074–14083.
39 N. Busschaert, M. Wenzel, M. E. Light, P. Iglesias-Hernández, R. Pérez-Tomás and P. A. Gale, *J. Am. Chem. Soc.*, 2011, **133**, 14136–14148.
40 S. Ko, S. K. Kim, A. Share, V. M. Lynch, J. Park, W. Namkung, W. Van Rossom, N. Busschaert, P. A. Gale, J. L. Sessler and I. Shin, *Nat. Chem.*, 2014, **6**, 885–892.
41 A. M. Rodilla, L. Korrodi-Gregório, E. Hernando, P. Manuel-Manresa, R. Quesada, R. Pérez-Tomás and V. Soto-Cerrato, *Biochem. Pharmacol.*, 2017, **126**, 23–33.
42 V. Soto-Cerrato, P. Manuel-Manresa, E. Hernando, S. Calabuig-Fariñas, A. Martinez-Romero, V. Fernández-Dueñas, K. Sahlholm, T. Knopfel, M. Garcia-Valverde, A. M. Rodilla, E. Jantus-Lewintre, R. Farras, F. Ciruela, R. Perez-Tomas and R. Quesada, *J. Am. Chem. Soc.*, 2015, **137**, 15892–15898.
43 N. Busschaert, S.-H. Park, K.-H. Baek, Y. P. Choi, J. Park, E. N. W. Howe, J. R. Hiscock, L. E. Karagiannidis, I. Marques, V. Félix, W. Namkung, J. L. Sessler, P. A. Gale and I. Shin, *Nat. Chem.*, 2017, DOI: 10.1038/NCHEM.2706.
44 X. Wu and P. A. Gale, *J. Am. Chem. Soc.*, 2016, **138**, 16508–16514.
45 H. J. Clarke, E. N. W. Howe, X. Wu, F. Sommer, M. Yano, M. E. Light, S. Kubik and P. A. Gale, *J. Am. Chem. Soc.*, 2016, **138**, 16515–16522.
46 I. Alfonso and R. Quesada, *Chem. Sci.*, 2013, **4**, 3009–3019.
47 C. R. Elie, G. David and A. R. Schmitzer, *J. Med. Chem.*, 2015, **58**, 2358–2366.
48 A. I. Share, K. Patel, C. Nativi, E. J. Cho, O. Francesconi, N. Busschaert, P. A. Gale, S. Roelens and J. L. Sessler, *Chem. Commun.*, 2016, **52**, 7560–7563.
49 B. Shen, X. Li, F. Wang, X. Yao and D. Yang, *PLoS One*, 2012, **7**, e34694.
50 P.-Y. Liu, S.-T. Li, F.-F. Shen, W.-H. Ko, X.-Q. Yao and D. Yang, *Chem. Commun.*, 2016, **52**, 7380–7383.

51 L. J. V. Galietta, P. M. Haggie and A. S. Verkman, *FEBS Lett.*, 2001, **499**, 220–224.
52 H. Li, H. Valkenier, L. W. Judd, P. R. Brotherhood, S. Hussain, J. A. Cooper, O. Jurček, H. A. Sparkes, D. N. Sheppard and A. P. Davis, *Nat. Chem.*, 2016, **8**, 24–32.
53 J. Shang, W. Si, Y. Che, J.-L. Hou and H. Jiang, *Org. Lett.*, 2014, **16**, 4008–4011.
54 M. Lisbjerg, H. Valkenier, B. M. Jessen, H. Al-Kerdi, A. P. Davis and M. Pittelkow, *J. Am. Chem. Soc.*, 2015, **137**, 4948–4951.
55 J. Mareda and S. Matile, *Chem. – Eur. J.*, 2009, **15**, 28–37.
56 R. E. Dawson, A. Hennig, D. P. Weimann, D. Emery, V. Ravikumar, J. Montenegro, T. Takeuchi, S. Gabutti, M. Mayor, J. Mareda, C. A. Schalley and S. Matile, *Nat. Chem.*, 2010, **2**, 533–538.
57 A. Vargas Jentzsch, D. Emery, J. Mareda, P. Metrangolo, G. Resnati and S. Matile, *Angew. Chem., Int. Ed.*, 2011, **50**, 11675–11678.
58 L. Adriaenssens, C. Estarella, A. Vargas Jentzsch, M. M. Belmonte, S. Matile and P. Ballester, *J. Am. Chem. Soc.*, 2013, **135**, 8324–8330.
59 A. Vargas Jentzsch, D. Emery, J. Mareda, S. K. Nayak, P. P. Metrangolo, G. Resnati, N. Sakai and S. Matile, *Nat. Commun.*, 2012, **3**, 905–912.
60 S. Benz, M. Macchione, Q. Verolet, J. Mareda, N. Sakai and S. Matile, *J. Am. Chem. Soc.*, 2016, **138**, 9093–9096.